ผลของโครงสร้างไทเทเนียมไดออกไซด์และการเติมโคบอลต์ต่อสมบัติในการเร่งปฏิกิริยาของตัวเร่งปฏิกิริยารูเทเนียมบนไทเทเนียมไดออกไซด์ในปฏิกิริยาไฮโดรจิเนชันแบบเลือกเกิดของเฟอร์ฟูรัลเป็นเฟอร์ฟูริลแอลกอฮอล์

นายณัฐดนัย นันทสันติ

วิทยานิพนธ์นี้เป็นส่วนหนึ่งของการศึกษาตามหลักสูตรปริญญาวิศวกรรมศาสตรมหาบัณฑิต
สาขาวิชาวิศวกรรมเคมี ภาควิชาวิศวกรรมเคมี
คณะวิศวกรรมศาสตร์ จุฬาลงกรณ์มหาวิทยาลัย
ปีการศึกษา 2560

EFFECTS OF TITANIUM DIOXIDE STRUCTURE AND COBALT ADDITION ON THE CATALYTIC PROPERTIES OF Ru/TiO_2 IN THE SELECTIVE HYDROGENATION OF FURFURAL TO FURFURYL ALCOHOL

Mr. Natdanai Nanthasanti

A Thesis Submitted in Partial Fulfillment of the Requirements
for the Degree of Master of Engineering Program in Chemical Engineering
Department of Chemical Engineering
Faculty of Engineering
Chulalongkorn University
Academic Year 2017

Thesis Title	EFFECTS OF TITANIUM DIOXIDE STRUCTURE AND COBALT ADDITION ON THE CATALYTIC PROPERTIES OF Ru/TiO_2 IN THE SELECTIVE HYDROGENATION OF FURFURAL TO FURFURYL ALCOHOL
By	Mr. Natdanai Nanthasanti
Field of Study	Chemical Engineering
Thesis Advisor	Professor Joongjai Panpranot, Ph.D.

Accepted by the Faculty of Engineering, Chulalongkorn University in Partial Fulfillment of the Requirements for the Master's Degree

.....Dean of the Faculty of Engineering

(Associate Professor Supot Teachavorasinskun, D.Eng.)

THESIS COMMITTEE

.....Chairman

(Professor Bunjerd Jongsomjit, Ph.D.)

.....Thesis Advisor

(Professor Joongjai Panpranot, Ph.D.)

.....Examiner

(Palang Bumroongsakulsawat, Ph.D.)

.....External Examiner

(Assistant Professor Okorn Mekasuwandumrong, D.Eng.)

ณัฐดนัย นันทสันติ : ผลของโครงสร้างไทเทเนียมไดออกไซด์และการเติมโคบอลต์ต่อสมบัติในการเร่งปฏิกิริยาของตัวเร่งปฏิกิริยารูเทเนียมบนไทเทเนียมไดออกไซด์ในปฏิกิริยาไฮโดรจิเนชันแบบเลือกเกิดของเฟอร์ฟูรัลเป็นเฟอร์ฟูริลแอลกอฮอล์ (EFFECTS OF TITANIUM DIOXIDE STRUCTURE AND COBALT ADDITION ON THE CATALYTIC PROPERTIES OF Ru/TiO_2 IN THE SELECTIVE HYDROGENATION OF FURFURAL TO FURFURYL ALCOHOL) อ.ที่ปรึกษาวิทยานิพนธ์หลัก: ศ. ดร. จูงใจ ปั้นประณต, 84 หน้า.

เฟอร์ฟูริลแอลกอฮอล์เป็นสารมัธยันตร์ที่มีความสำคัญในการผลิตสารเคมีมูลค่าสูงที่สำคัญหลายชนิด โดยทั่วไปเฟอร์ฟูริลแอลกอฮอล์ผลิตจากปฏิกิริยาไฮโดรจิเนชันของเฟอร์ฟูรัลที่ได้จากชีวมวลจากพืชโดยใช้ ตัวเร่งปฏิกิริยาโลหะที่มีตัวรองรับ งานวิจัยนี้เตรียม ๑.๕ เปอร์เซ็นต์โดยน้ำหนักของ รูเทเนียม บนตัวรองรับไทเทเนียมไดออกไซด์ ด้วยวิธีการเคลือบฝังและศึกษาผลของโครงสร้างผลึกของไทเทเนียมไดออกไซด์และการเติมโคบอลต์ปริมาณ ๐.๒ ถึง ๐.๘ เปอร์เซ็นต์โดยน้ำหนัก ในปฏิกิริยาไฮโดรจิเนชันแบบเลือกเกิดของเฟอร์ฟูรัลเป็นเฟอร์ฟิวริวแอลกอฮอล์ที่ อุณหภูมิ ๕๐ องศาเซลเซียส ความดันไฮโดรเจน ๒๐ บาร์ และเวลาการทำปฏิกิริยา ๒ ชั่วโมง พบว่าการใช้ไทเทเนียมไดออกไซด์ที่มีโครงสร้างผลึกแบบอนาเทสเป็นตัวรองรับโลหะรูเทเนียมให้ ค่าการเปลี่ยนแปลงของเฟอร์ฟูรัล และค่าการเลือกเกิดเป็นเฟอร์ฟิวริวแอลกอฮอล์ ที่ดีที่สุดที่ ๓๒ เปอร์เซ็นต์ และ ๙๐ เปอร์เซ็นต์ตามลำดับ เนื่องจากไทเทเนียมไดออกไซด์อนาเทสช่วยสนับสนุนการดูดซับไฮโดรเจนที่มากกว่าไทเทเนียมไดออกไซด์รูไทล์ การเติมปริมาณโคบอลต์ปริมาณเล็กน้อยลงในตัวเร่งปฏิกิริยารูเทเนียมบนตัวรองรับไทเทเนียมไดออกไซด์อนาเทส ช่วยเพิ่มประสิทธิภาพของตัวเร่งปฏิกิริยาและเพิ่มค่าการเลือกเกิดของเฟอร์ฟูริลแอลกอฮอล์โดยที่ ๑.๕ เปอร์เซ็นต์รูเทเนียม ๐.๖ เปอร์เซ็นต์โคบอลต์ บนตัวรองรับไทเทเนียมไดออกไซด์ แสดงผลที่ดีที่สุดของ ตัวเร่งปฏิกิริยาที่ ๙๒ เปอร์เซ็นต์ของค่าการเปลี่ยนแปลงของเฟอร์ฟูรัล และ ๙๗.๕ เปอร์เซ็นต์ของค่าการเลือกเกิดเฟอร์ฟูริลแอลกอฮอล์ คาดว่าการเติมโคบอลต์ส่งผลให้ ขนาดของโลหะผสมใหญ่ขึ้นและช่วยเพิ่มอันตรกิริยาระหว่างรูเทเทียมกับโคบอลต์ ซึ่งสอดคล้องกับการวิเคราะห์คุณลักษณะของตัวเร่งปฏิกิริยาด้วยกล้องจุลทรรศน์อิเล็กตรอนแบบส่องผ่าน การรีดักชันของไฮโดรเจนด้วยการโปรแกรมอุณหภูมิ และ เอ็กซเรย์โฟโตอิเล็กตรอนสเปกโตรสโกปี

ภาควิชา วิศวกรรมเคมี ลายมือชื่อนิสิต .....

สาขาวิชา วิศวกรรมเคมี ลายมือชื่อ อ.ที่ปรึกษาหลัก .....

ปีการศึกษา 2560

5970157621 : MAJOR CHEMICAL ENGINEERING
KEYWORDS: FURFURAL / CATALYSTS / HYDROGENATION / FURFURAL HYDROGENATION / RUTHENIUM

NATDANAI NANTHASANTI: EFFECTS OF TITANIUM DIOXIDE STRUCTURE AND COBALT ADDITION ON THE CATALYTIC PROPERTIES OF Ru/TiO_2 IN THE SELECTIVE HYDROGENATION OF FURFURAL TO FURFURYL ALCOHOL. ADVISOR: PROF. JOONGJAI PANPRANOT, Ph.D., 84 pp.

Furfuryl alcohol, an important intermediate for the production of many fine chemicals, is typically produced by the selective hydrogenation of lignocellulosic biomass-derived furfural using supported metal catalysts. In this research, 1.5%wt Ru catalysts supported on nanocrystalline TiO_2 were prepared by incipient wetness impregnation method. The effects of crystallographic of TiO_2 and Co addition in the range of 0.2-0.8 wt% on the catalytic properties of Ru/TiO_2 were investigated in the selective hydrogenation of furfural to furfural alcohol at 50°C, 20 bar of H_2, and 2 h reaction time. It was found that Ru supported on anatase phase TiO_2 exhibited the highest conversion of furfural and selectivity of furfurly alcohol at 32 and 90%, respectively. The anatase phase of TiO_2 may promote adsorption of hydrogen atoms than rutile. The addition of a small amount of Co in the Ru/TiO_2 anatase improved the catalytic activity and furfurly alcohol selectivity with the $1.5\%Ru\text{-}0.6\%Co/TiO_2$ showed the best catalytic performances with 92% conversion of furfural and 97.5% furfurly alcohol selectivity. It is suggested that Co addition increased the Ru-Co particles size and enhanced the interaction between Ru and Co as shown by the TEM, H_2-TPR, and XPS results.

Department: Chemical Engineering Student's Signature .....
Field of Study: Chemical Engineering Advisor's Signature .....
Academic Year: 2017

ACKNOWLEDGEMENTS

Foremost, I would like to express my sincere gratitude to my advisor Prof. Dr. Joongjai Panpranot for the continuous support of my Master study and research, for her invaluable guidance, suggestion, enthusiasm, and motivation. She was always open whenever I run into a trouble spot or had a question about my research or writing. She steered me in the right the direction whenever she thought I needed it so this thesis would not have been completed without her support. Moreover, I would also be appreciate to Asst. Prof. Dr. Okorn Mekasuwandumrong for good teaching and advice during research preparation and discussion. In additional, I would grateful to thank to Prof. Dr. Bunjerd Jongsomjit, as the chairman, Dr. Palang Bumroongsakulsawat, as a member of the thesis committee and for your very important comments on this thesis. Finally, I must express my very profound gratitude to my parents and to my friends for providing me with unfailing support and continuous encouragement throughout my years of study and thorough the process of researching and writing this thesis. I would like to thank acknowledge financial support from the Thailand Research Fund (TRF) and the Ratchadaphiseksomphot Endowment Fund for International Research Integration: Chula Research Scholar are gratefully acknowledged.

CONTENTS

Page

Page

Page

FIGURE CONTENTS

TABLE CONTENTS

CHAPTER I
INTRODUCTION

1.1 Introduction

At present, new technologies for the production of bio fuels as renewable energy received much interest by many researchers. This trend is popular due to energy-shortage problem, global warming, the depletion of fossil energy, and increasing pollution problems. Bio fuels and green chemicals can be obtained from biomass, which is considered as an important feedstock for the production [1]. Furfural is a green chemical that can be produced from xylose conversion of lignocellulosic biomass. It can also be found in the decomposition of agricultural waste such as wood, grass, and corncobs [2, 3]. The furfural hydrogenation has many pathways in this reaction, it can produce furfuryl alcohol, furan, 2-methylfuran, 2-methyl tetrahydrofuran, and tetrahydrofurfuryl alcohol, but the progressively interesting high value chemical is furfuryl alcohol [4]. Furfuryl alcohol (FA) has wide applications in the production of tetrahydrofurfuryl alcohol, polymers, resin, fibers, lysine, vitamin C, lubricants, and chemical intermediates for the production of perfume and vitamin [1, 5]. Conventional selective hydrogenation of furfural is carried out in liquid phase using copper chromite catalysts at high temperature and high pressure using batch reactor. The results show high conversion and selectivity for furfural hydrogenation but copper chromite has toxicity due to the presence of chromium which is another drawback. The toxicity of chromium can severely affect to the environment, which can cause to poisonous pollution [5, 6].

Noble metals have been considered as active catalysts to substitute the use of copper chromite catalysts because noble metals such as Pt, Pd, and Ru did not affect the environment and have high efficiency in the liquid-phase selective hydrogenation reactions [7]. The phase of titania support structure was found to significantly affect the hydrogenation reaction. The Ni/TiO_2 catalysts on anatase phase is higher activity than the rutile titania supported ones in the hydrogenation of p-nitrophenol to p-aminophenol because the titania structure has favorable influenced

the physio-chemical properties of the catalysts [8]. The Pd–Ru/TiO_2 catalyst in selective hydrogenation of furfural at room temperature and low pressure showed high selectivity towards 2-methylfuran and furfuryl alcohol by using the polar solvent [7]. The Ru/C and Pd/C catalysts have been investigated in the furfural hydrogenation, the results showed that the Pd/C catalyst demonstrated high efficiency for the reaction but Ru/C had low efficiency [6]. On the other hand, improving performance of the Ru catalyst was studied by bimetallic Pd-Ru/TiO_2 in furfural hydrogenation, the result displayed that the increasing of Ru content in the Pd increased the selectivity of 2-methylfuran and furfuryl alcohol but decreased the conversion [7]. Non-noble metal was inquired to improve the Ru catalyst. The addition of Sn to Ru catalysts aggressively appended the C=O bond of furfural hydrogenation and furfuryl alcohol selectivity [9].

In this work, the Ru catalyst supported on various phases of titania supports and the bimetallic Ru-Co catalysts supported on anatase phase titania were tested in the selective hydrogenation of furfural to furfuryl alcohol.

1.2 Research objectives

To investigate the characteristics and catalytic properties of TiO_2 supported Ru nanoparticles prepared with different phases of TiO_2 in the liquid-phase furfural hydrogenation.

To study the effect of bimetallic Ru-Co nanoparticles supported on TiO_2 anatase phase catalyst in liquid-phase furfural hydrogenation.

1.3 Research scopes

1. Titanium dioxide support with different phase (Rutile, Anatase, P25, and Sol-gel method) were used
2. Titanium dioxide support were prepared using sol-gel method and calcined at 350^{o}C under air atmospheres for 2 h

3. 1.5 wt% Ru/TiO_2 monometallic catalysts with different phases of TiO_2 supports and SiO_2 support were prepared by using incipient wetness impregnation method and calcined at 550°C under air atmospheres for 4 h
4. The reduction conditions were H_2 flow (25cm^3/min) at 300°C for 2 h
5. The bimetallic 1.5 wt% Ru and different amounts of Co (0.2, 0.4. 0.6, 0.8 wt%) supported on anatase phase TiO_2 were prepared by using incipient wetness impregnation method and calcined at 550°C under air atmospheres for 4 h
6. The catalysts were tested in the liquid phase furfural hydrogenation at 50°C and 2 MPa hydrogen pressure for 2 h
7. The catalysts were characterized by using X-ray diffraction (XRD), BET surface area, Hydrogen Temperature-programmed reduction (H2-TPR), X-ray photoelectron spectroscopy (XPS), CO-pulse chemisorption (CO-Chem), transmission electron microscopy (TEM), and Inductively coupled plasma-atomic emission spectrometry (ICP)

CHAPTER II
BACKGROUND AND LITERATURE REVIEWS

2.1 TiO_2 Support

Titania or titanium (IV) dioxide is the naturally appearing oxide of titanium. The chemical formula of titania is TiO_2, it is used as white pigment. The most popular titania used as support for catalyst in many industrials is P-25, it is also universally used in heterogeneous catalysis reactions such as photo degradation, oxidation, and hydrogenation because it has commercial availability, excellent stability for chemicals, and low price. It has wide range of applications such as production of paint, food coloring, plastics, fibers, electronic, sunscreen lotions, solar cells, capacitors and rubber. Titania mainly exists in both crystalline and amorphous forms and different crystalline phases for example anatase, rutile, and brookite phase (**Figure 2.1**). The crystallite size of rutile is larger than anatase and it has high thermally stable. Brookite is infrequently utilized. Moreover, anatase and brookite phase can convert to rutile phase at temperature above 600°C. The anatase phase has a tetragonal crystal structure (with dipyramidal habit) and contains zigzag chains of octahedral molecules linked while the rutile phase has a tetragonal crystal structure (with prismatic habit) and contains linear chains of opposite edge-shared octahedral structure. The brookite phase has an orthorhombic crystalline structure (**Table 2.1**). The morphologies of TiO_2 exist as nanostructures, for examples, nanotubes, nanowires, nanorods, and mesoporous structures [10]. The synthetic methods of TiO_2 include sol-gel method, solvothermal method, chemical vapor deposition, electrodeposition, and direct oxidation method.

Table 2.1 Crystal structure of TiO_2 [11, 12]

Properties	Anatase	Brookite	Rutile
Crystal structure	Tetragonal	Orthorhombic	Tetragonal
Density, kg/m^3	3790	3990	4130
Molecule (cell)	2	2	4
Space group	$P4_2/mnm$	$I4_1/amd$	Pbca
Lattice constant (Å)			
a	3.784	9.184	4.594
b	-	5.447	-
c	9.515	5.154	2.959
Ti-O bond length (Å)	1.949 (4) 1.980 (2)	1.937 (4) 1.965 (2)	1.87-2.04
O-Ti-O bond angle	81.2° 90.0°	77.7° 92.6°	77.0°-105°

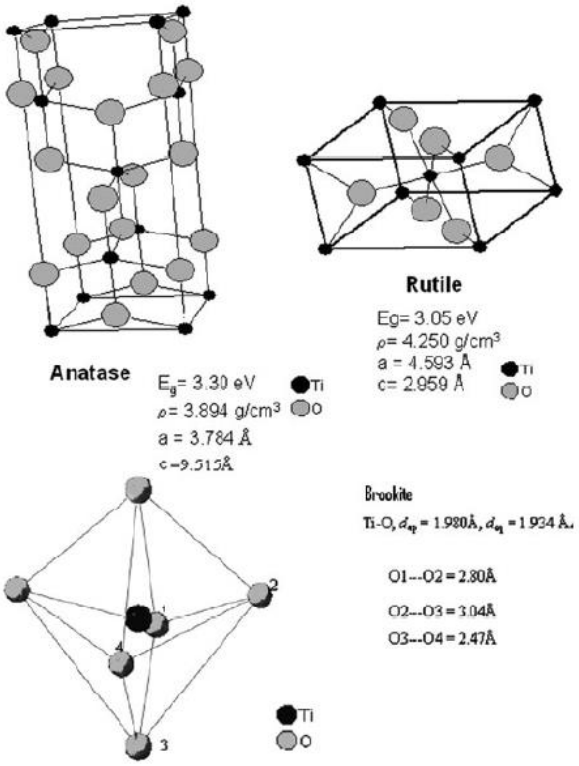

Figure 2.1 Different forms of TiO_2

TiO_2 possesses high physical and chemical stability and it has abundant element and transition metal such as Titanium (III) and titanium (IV), which is normal oxidation states of TiO_2 element [13]. TiO_2 based catalysts are interested in heterogeneous catalysis because of its nontoxicity, high effectiveness, good mechanical resistance, stability in acidic and oxidative environments, and various oxidation states of TiO_2 element for the applications in selective, catalytic oxidation of organic compounds, polymerization catalysis, photocatalysis, and hydrogenation catalysis [13]. The disadvantage of TiO_2 is small specific surface areas, low quantum efficiency, and low adsorption, and low adsorption abilities [14].

2.2 Strong interaction between metal and support

The strong metal-support interaction (SMSI) occurs on the group VIII metals supported on reducible oxide supports reduced at high temperatures. The strong interaction between the metal and TiO_2 improved catalytic stability and activity. Wang, S-Y. et al. [15] studied the activity of Pd in methanation reaction. This research showed that Pd on TiO_2 support is the most active catalyst but silica-supported Pd is the least active resulting from the SMSI of metal and TiO_2 support. The Pd/TiO_2 had the highest turnover frequencies based on the chemisorption and the more competitive hydrogen chemisorption. Pereira, M.M. et al. [16] reported the strong suppression of H_2 and CO chemisorption on a group VIII metal supported on a reducible oxide. It was interesting that at high temperature reduction affected on the structure sensitive reaction. In this research, the bimetallic Pd-Cu on TiO_2 was prepared by incipient wetness impregnation and studied in the 1, 3-butadiene hydrogenation. The hydrogen chemisorption and turnover frequency were decreased because of the SMSI effect, which resulted by the reduction at high temperature.

2.3 Ruthenium catalyst

Ruthenium is a chemical element with symbol Ru, atomic number 44 and the 4d transition metals. Ruthenium has the range 0 to +8 oxidation states but the normal

state is +2, +3, and +4. It is a rare transition metal belonging to the platinum group and is in group 8 of the periodic table and inert to most other chemicals. Ruthenium was used in wear-resistant electrical contacts and chemistry catalyst. Moreover, it is in platinum alloys because Small amounts of ruthenium can increase the hardness of platinum and palladium. The small amount of ruthenium was increased the corrosion resistance of titanium

The selective hydrogenation was popular investigated by transition metal nanoparticles such as Pt, Pd, Cu, Ni, Ru, Au, and Fe because they have metal surface activation and catalysis selectivity. Cui, X. et al. [17] used ruthenium nanoparticles (Ru-NPs) for selective hydrogenation at C=O bond of aromatic rings because it is low cost metal catalyst compared with other noble metals but the result of ruthenium catalyst showed high activity and selectivity for hydrogenation of all kinds of substituted arenes including lignin-derived aromatic compounds. In this research, prepared Ru nanoparticles supported on a nitrogen-doped carbon material were prepared and tested in hydrogenation of aromatic ethers to the corresponding alicyclic compounds with preservation of the phenyl- and benzyl C–O bonds. The Ru noble metal catalyst plays a pivotal role in the reaction under mild conditions.

2.4 Cobalt catalyst

Cobalt is a chemical element with symbol Co and atomic number 27. It has only in chemically combined form and has been used for jewelry and paints. The metallic-lustered ores such as cobaltite and the by-product of copper and nickel mining were used to produce cobalt. The main product that prepare by cobalt for example magnetic, wear-resistant and high-strength alloys. Cobalt is a ferromagnetic metal with a specific gravity of 8.9 and the metallic form has two crystallographic structures: hcp and fcc. The advantage in catalyst field of cobalt that has weakly reducing metal and passivating oxide film plays role by protect from oxidation. Cobalt has +2 and +3 of common oxidation states from ranging -3 to +5. The cobalt was active at high operating condition, Mansouri, M. et al. [18] used cobalt-based catalysts as for hydrocarbon synthesis, it has the FTS activity, and selectivity for long-chain paraffins.

The $Co/K/Al_2O_3$ catalyst was prepared by impregnation with an aqueous solution on Fischer–Tropsch synthesis. FTS was carried out in a fixed-bed micro-reactor at temperature of 483–513 K, pressure of 8bar, H2/CO feed ratio of 1–3, and space velocity of 2700–5200 h^{-1}. The 15wt.%Co/10wt.%K/Al_2O_3 is the optimal amount of catalyst. Moreover, improving of catalytic activity of cobalt was synthesized the bimetallic catalysts from Silva, Rosenir R.C.M. et al. [19] studied the cobalt based catalyst on various supports for hydrogen production. Co catalyst showed lower activity in this reaction but it did not have an induction period. It is popular to prepare Co bimetallic catalysts with other metals in catalyst research field. Co is necessary to promote Ni to increase the particle size. Methane decomposition for hydrogen production via accumulation of carbon by cobalt catalysts with silica, alumina, and niobia support, the Co/SiO_2 reduced at 300°C showed the increased conversion with reaction time. The Co/SiO_2 reduced at 500°C was the best catalyst for methane decomposition and the catalyst was observed a rapid sintering of the metal particles because of the drop in hydrogen chemisorption.

2.5 Furfural hydrogenation

Hydrogenation is a chemical reaction between molecular hydrogen and another compound or element to reduce double and triple bonds in hydrocarbons such as alkene, the reaction is usually used with catalyst to reduce the reaction temperature and pressure such as platinum, copper, and palladium. The hydrogenation reaction occurs from the addition of pairs of hydrogen atoms to a molecule. The step of hydrogenation of a C=C double bond at a catalyst surface consists of 3 main steps (1) the hydrogen adsorbs to the catalyst surface to form adsorbed H atoms (2) the reactant adsorbs to the catalyst surface, and (3) the reactant reacts with adsorbed H atoms to give the product and the molecule leaves the surface.

Heterogeneous catalysis consists of catalyst in a different phase from reactants and the catalyst usually composes of metal and support. Metal nanoparticles with high surface area provide a good basis for the molecular design of mixed oxide catalysts**.** The advantage of heterogeneous catalysis is easy separation of the catalyst

from the product and the catalyst can be recycled. The heterogeneous catalysis has high thermal stability and hydrolytic stability in solution, it can operate at high temperature [20].

Furfuryl alcohol was produced by furfural hydrogenation in liquid or vapor phase by the heterogeneous catalysis reaction. The investigation of the hydrogenation of the C=O bonds on the furan rings [9] is shown in **Figure 2.4**. The catalysts usually used in furfural hydrogenation are Ni, Cu, Fe, Co, and noble metals group VIII (Pt, Pd, and Ru) because they can reduce the carbonyl group. The reaction was operated with organic solvents, for examples, octane, methanol, ethanol, and 2-propanol but water is preferred due to environmental issue [21]. Furfural was produced from xylose by bio-derivative and product of furfural by noble metal supported on TiO_2 in liquid phase hydrogenation into furfuryl alcohol, tetrahydrofurfural, tetrahydrofuran, and tetrahydrofurfuryl alcohol, as shown in **Figure 2.2**. The main product that is focused in this reaction is furfuryl alcohol. It is a substance that have many applications in the chemical industry such as fine chemicals, polymers, tetrahydrofurfuryl alcohol, 2,3-dihydropyran, resin, fibers, lysine, vitamin C, lubricants adhesives, and wetting agents as shown in **Figure 2.3** [7].

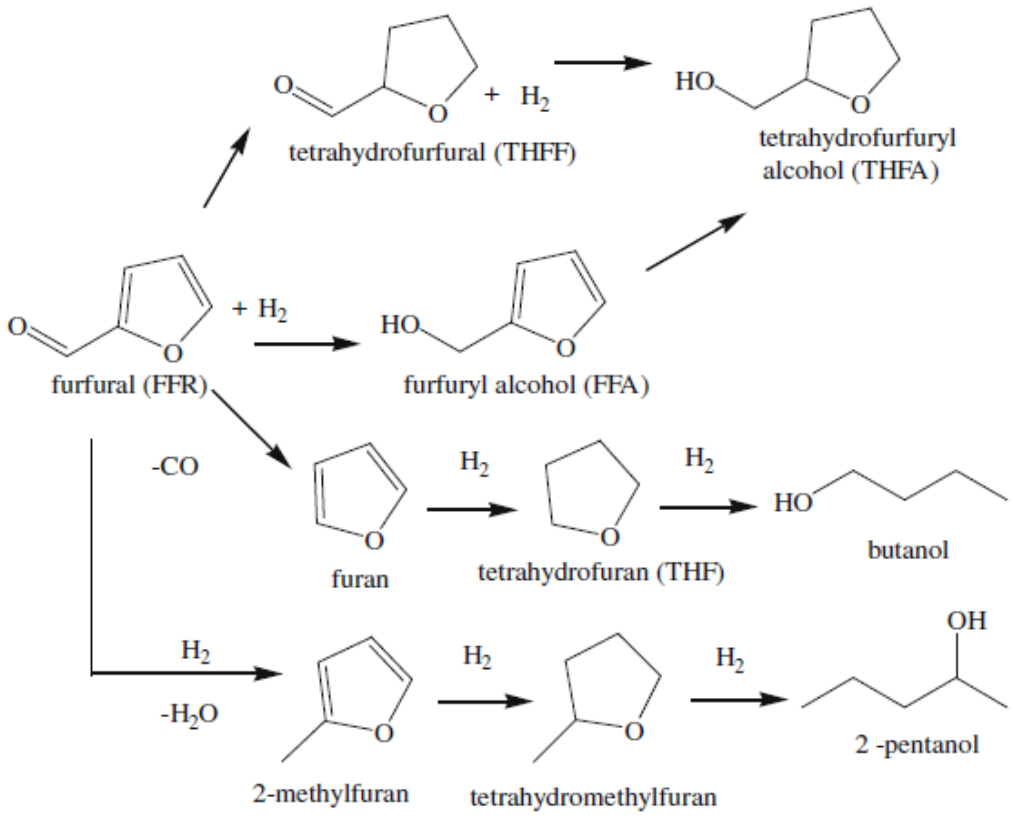

Figure 2.2 The pathways of furfural hydrogenation [9]

Figure 2.3 The applications of furfuryl alcohol

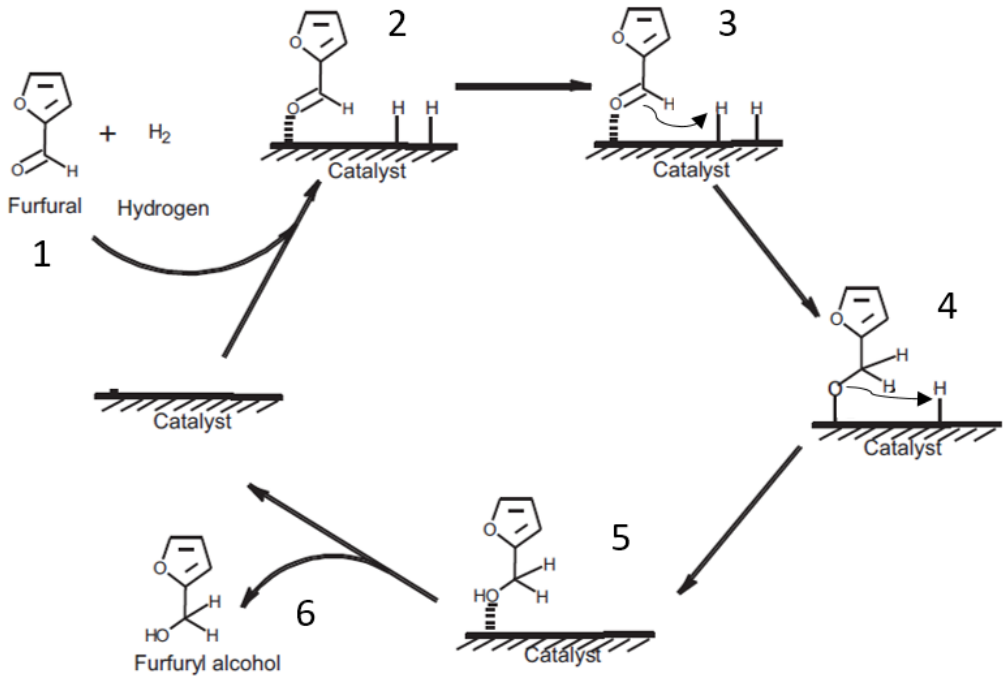

Figure 2.4 The mechanism for the hydrogenation of furfural to furfural alcohol [22]

Table 2.2 Summary of the research of the furfural hydrogenation on various catalysts under different reaction conditions.

Ref.	Purposes of study	Catalysts and preparation methods	Reaction conditions	Results
Chen, H. et al. (2018) [23]	Studied the effects of the Cu state supported on $MgO-Al_2O_3$ catalysts in the hydrogenation of furfural to furfuryl alcohol	$Cu/MgO-Al_2O_3$ (10-50wt% Cu loading) by co-precipitation and calcined at 450°C for 2 h	-Liquid phase -Reduce at 450°C for 2h -Furfurl 100 mg, catalyst 25 mg, temperature 210°C, time 1 h, pressure 1 atm, isopropanol 5 mL	-The best performance is 20%Cu/ $MgO-Al_2O_3$ -The optimal time is 1h - Excellent stability after four cycles of catalyst

Ref.	Purposes of study	Catalysts and preparation methods	Reaction conditions	Results
Vargas-Hernández, D. et al. (2014) [24]	Studied the effects of the Cu spported on SBA-15 silica catalysts and compared with copper chromite for the hydrogenation of furfural to furfuryl alcohol	Cu/SBA-15 silica (8, 15, 20wt% Cu loading) by impregnation and calcined at 400°C for 6 h	-Vapor phase -Reduce at 350°C for 2h -Catalyst 150 mg, temperature 170°C, H2 flow 10 ml/min, feed flow 2.3 mmol/h	- 15%wtCu/SBA-15 catalyst shows the highest activity and selectivity at 170 °C - All catalysts undergo deactivation with time on stream -All Cu/SBA-15 catalysts better than copper chromite
Sharma, R. V. et al. (2013) [22]	Developed the Cu:Zn:Cr:Zr based catalysts for the hydrogenation of furfural to furfuryl alcohol	Prepare by Co-precipitation method	-Liquid phase -Reduce at 300°C for 2h -Furfurl 12.43mL, catalyst 1.5 g, temperature 170°C, time 3 h, pressure 2MPa, isopropyl alcohol 87.57mL	-The addition of Zn increases the activity of the catalyst, increased the acidity, and helped in the dispersion of metallic Cu

Ref.	Purposes of study	Catalysts and preparation methods	Reaction conditions	Results
Villaverde, M.M. et al. (2013) [25]	Studied the different Cu-based catalysts for the hydrogenation of furfural to furfuryl alcohol	Cu/SiO2-I by incipient wetness impregnation and decomposed in N_2 flow at 400°C for 5 h - Cu/SiO2-PD by precipitation–deposition and decomposed in N2 flow at 400°C for 5 h - CuMgAl, CuZnAl and Cu-Cr by co-precipitation and decomposed in N2 flow at 500°C for 5 h	-Liquid phase -Reduce at 400°C for 1.5h -Furfurl 0.25–1.00 mL, catalyst 0.1 g, temperature 110°C, time 1 h, pressure 1MPa, 2-propanol 60mL	-The best catalyst is CuMgAl catalyst -A solid catalyst formed by small copper particles is more active and stable

Ref.	Purposes of study	Catalysts and preparation methods	Reaction conditions	Results
Bhoges wararao , S. et al. (2015) [26]	Studied the differences in structure and mode of furfural adsorption of Pt and Pd metal supported on γ-Al_2O_3 for furfural hydrogenation	Pd (2, 5, and 10wt%)/Al_2O_3 by wet impregnation method and calcined at 400°C for 2 h Pt (2, 5, and 10wt%) on Al_2O_3 , SO_4–ZrO_2, MgO and SiO_2 support by wet impregnation method and calcined at 400°C for 2 h	-Liquid phase -Pd Reduce at 250°C for 2.5h -Pt Reduce at 350°C for 2.5h -Furfurl 1g, catalyst 0.05 g, temperature 25-240°C, time 0.5-8 h, pressure 0.5-3MPa, solvent 20mL Iso-propanol, toluene, water and mixtures of iso-propanol–water (1:1, 2:1, and 4:1 weight ratio) and toluene–water (4:1 weight ratio)	-Furfural was hydrogenated at 25°C -Pt catalysts were selective for hydrogenation of C=O group -Pd catalysts hydrogenated both ring and C=O groups of FAL yielding FOL and THFOL -At temperature higher than 180°C the Pd catalysts enabled decarbonylation of FAL to furan and the Pt catalysts facilitated hydrogenolysis of C=O and C-O groups enabling 2-MF and furan

Ref.	Purposes of study	Catalysts and preparation methods	Reaction conditions	Results
O'Driscoll, Á. et al. (2017) [27]	Synthesised of monometal-lic catalysts by wet impregnation and concentrated on the employment of metals for the liquid phase hydrogenation	1%wtCu, 1%wt Ni, 1%wt Pd, 1%wt Pt, 2%wt Cu, 2%wt Ni, 2%wt Pd, and 2%wt Pt on SiO_2 support by wet impregnation method and calcined at 450°C for 5 h	-Liquid phase -Reduce at 300°C for 4h -Furfurl 25 mL, catalyst 1g, temperature 100°C, time 1 h, pressure 2MPa, ethanol 175mL	-SiO_2 support was the best furfuryl alcohol selectivity -Pt metal was the highest selectivity to furfurylalcohol

The research of furfural hydrogenation over the catalysts has become increasingly popular at present because the current of biomass fuels and chemicals. Reaction conditions, metals, supports, preparing methods, and required products have been varied. The Cu metal was popular to investigate in the furfural hydrogenation. Chen, H. et al. (2018) [23] studied the effect of the Cu state supported on MgO-Al_2O_3 catalysts in the hydrogenation of furfural to furfuryl alcohol. From the results, it is suggested that the effect of the Cu state on Cu/MgO-Al_2O_3 achieved a high catalytic activity and 20%Cu/MgO-Al_2O_3 showed the high yield of furfuryl alcohol because of the strongly dependent on the copper content, the balance between the Cu loading and dispersion, and the completely reduction of surface Cu^{2+} to Cu^2. The state of Cu^0 showed better dispersion of nanoparticles, a higher reduction degree of Cu, and stronger adsorption of furfural can contribute to high hydrogenation performance. The decrease in the amount of Lewis acidity also increased the performance of catalysts.

The temperature and time had a significant effect on the conversion and the best condition was 210°C for 1 h but it was unstable. The furfuryl alcohol has been produced stably at 170 and 190°C without other products or degradation. O'Driscoll, Á. et al. (2017) [27] synthesised of monometallic catalysts by wet impregnation and concentrated on the employment metals for the liquid phase hydrogenation. The SiO_2 support displays higher furfural conversion because of high surface area and high actual metal loading.

The superior metal for furfuryl alcohol production is platinum based catalysts because platinum is noble metal and it is structure selective to hydrogenate the C=O bond at high furfural conversion. Vargas-Hernández, D. et al. (2014) [24] studied the effects of the Cu spported on SBA-15 silica catalysts and compared with copper chromite for the hydrogenation of furfural to furfuryl alcohol. It was found that the presence of Cu^0-Cu^+ species on the catalyst surface is responsible for the high activity and selectivity toward furfuryl alcohol. The SBA-15Cu showed high activity and selectivity toward the desired product at 170 °C and all the SBA-15 silica catalysts showed higher activity than copper chromite because the SBA-15silica has more surface area and the SBA-15Cu catalyst has higher activity than SBA-20Cu resulting from lacking of required number of smaller Cu particles that makes the SBA-20Cu catalyst less active in furfural hydrogenation. Sharma, R. V. et al. (2013) [22] developed the Cu:Zn:Cr:Zr based catalysts for the hydrogenation of furfural to furfuryl alcohol. From the results, it was found that the addition of Zn increases the activity for furfural conversion and the addition of Zr increases selectivity by reducing the crystalline size of the Cu. The increasing of Zr content grain the acidity of the catalyst and helps in the dispersion of Cu particles. The novel Cu(3):Zn(2):Cr(1):Zr(3) catalyst is the optimum ratio for this reaction. Villaverde, M.M. et al. (2013) [25] studied the different support on Cu-based catalysts for the hydrogenation of furfural to furfuryl alcohol, which prepared by the incipient wetness impregnation (Cu/SiO_2-I), precipitation–deposition (Cu/SiO_2-PD), and co-precipitation (CuMgAl, CuZnAl and Cu-Cr) methods. The highest activity of CuMgAl was resulted from interaction between Cu^0 atoms and Mg^{2+}cations and high Cu dispersion and H_2 chemisorption capacity. In the reaction, high

temperature makes high furfural conversion rates and reduces deactivation. The metals used in previous studies were non-noble metals but Bhogeswararao, S. et al. (2015) [26] studied the noble metal on the differences in structure and mode of furfural adsorption of Pt and Pd metal supported on γ-Al_2O_3 for furfural hydrogenation. Excellent activity at room temperature of Pt and Pd catalysts was observed. At high temperature, the Pd catalyst showed expertly decarbonylation activity forming furan because Pd catalyst is selective for C=O hydrogenation. The polar sovent led to high conversion of furfural. The supported Pt catalysts show hydrogenolysis of C=O and C-O groups enabling 2-methylfuran and furan ring-opened products.

2.6 The effect of titania support on hydrogenation reaction

Table 2.3 Summary of the research on the effect of titania structure support for hydrogenation reaction.

Ref.	Purposes of study	Results
Rizhi, C. et al. (2006) [8]	Studied the titania structure on Ni/TiO_2 Catalysts prepared by a liquid-phase chemical reduction method for hydrogenation of p-nitrophenol to p-aminophenol	- The titania structure has significant influence on the dispersion, particle size and reduction behavior -The activity of TiO_2 anatase phase is higher than TiO_2 rutile
Li, Y. et al. (2004) [28]	Studied the strong metal-support interaction by the effect of titania polymorph for the liquid phase selective hydrogenation of long chain alkadienes	-The anatase titania shows that even pre-reduced by H_2 at lower temperature and high selectivity of alkenes -The rutile titania is more thermodynamically and structurally stable -The surface lattice of anatase easier to diffuse to surface of palladium particle
Panpranot, J. et al. (2006) [29]	Studied the TiO_2 supports consisting of various crystalline phase in Selective Acetylene Hydrogenation	-The increasing rutile phase shows the decreasing in Brunauer-Emmett-Teller surface areas, fewer Ti^{3+} sites, and lower Pd dispersion -The optimum rutile containing is 44%

The titania is the most popular in the hydrogenation reaction due to the different crystalline phases, low price, nontoxicity, commercial and excellent stability for chemicals. Rizhi, C. et al. (2006) [8] studied the titania structure on Ni/TiO_2 catalysts

prepared by a liquid-phase chemical reduction method for hydrogenation of p-nitrophenol to p-aminophenol. From the results, it was found that the titania structure has favorable influence on physio-chemical and catalytic properties of Ni/TiO_2 catalysts and the anatase phase of titania shows higher activity than rutile phase of titania because the nickel oxide is easy to reduce to metallic nickel on anatase phase of titania similar to under reaction conditions. For the different crystalline phases of titania, the mixed crystalline phases of titania was investigated by Panpranot, J. et al. (2006) [29], the TiO_2 supports consisting of various crystalline phases were studied in selective acetylene hydrogenation. From the results, the rutile phase titania displayed the best efficiency of catalyst for the selective acetylene hydrogenation because of the Increasing percentages of rutile phase in the TiO_2 showed the dropping of Brunauer-Emmett-Teller surface areas, fewer Ti^{3+} sites, and lower Pd dispersion. The increasing of ethylene resulted from Ti^{3+} in contact with Pd can probably lower the adsorption strength of ethylene. In addition, the SMSI effect of the titania was important to the hydrogenation reaction. Li, Y. et al. (2004) [28] studied the strong metal-support interaction by the effect of titania polymorph for the liquid phase selective hydrogenation of long chain alkadienes. From the results, it was found the reduction by H_2 of anatase titania catalyst occurs at low temperature but rutile phase has high temperature reduction and rutile phase is more thermodynamically and structurally stable than anatase titania because Ti^{3+} ions in the surface lattice of anatase phase is easy to diffuse to surface of metal particle.

2.7 The noble metal ruthenium catalyst on furfural hydrogenation

Table 2.4 Summary of the research on the ruthenium catalyst on furfural hydrogenation with different supports and reaction conditions.

Ref.	Purposes of study	Catalysts and preparation methods	Reaction conditions	Results
Panagiotopoulou, P. et al. (2014) [30]	Studied the effect of alcohol hydrogen donor on methyl furan production by Ru/C catalyst	5%wt $Ru/RuO_2/C$ by Sigma–Aldrich	-Liquid phase -Reduce at 300°C for 3h -Furfurl 1%wt in solvent, catalyst 0.1 g, temperature 180°C, time 5 h, pressure 2 MPa, alcohol 24 mL	-The Ru/RuO2/C catalyst is capable of complete furfural conver-sion and high MF yield -Secondary alcohols are more effective in CTH
Mironenko, R M. et al. (2015) [6]	Studied the formation and catalytic properties of the active sites in Pd/C and Ru/C catalysts for hydrogenation of furfural	-1.5wt%Ru/C and 1.5%wtPd/C by incipient wetness impregnation of thecarbon supports (CB, CNT) and calcined at 550°C	-Liquid phase -Reduce at 250°C for 2h -Furfurl 5 mL, catalyst 0.5 g, temperature 50°C, time 0.5 h, pressure 0.5 MPa, distilled water 60 mL	-Pd/CNT are reduced at a lower temperature -The 1.5% Pd/CB catalyst demonstrated a high selectivity

Ref.	Purposes of study	Catalysts and preparation methods	Reaction conditions	Results
Panagiotopoulou, P. et al. (2014) [31]	Studied the methyl furan production by hydrogenation of furfural in the liquid phase on Ru/C catalyst	5%wt Ru/C by Sigma–Aldrich	-Liquid phase -Reduce at 300°C for 3h -Furfurl 1wt% in solvent, catalyst 0.1 g, temperature 50°C, time 5 h, pressure 2MPa, 2-propanol 24 mL	-The optimum condition is 10 h of reaction at 180°C -The catalyst recycling does not decrease significantly
Yang, J. et al. (2016) [32]	Studied the effect of aromatic and aliphatic organic linkers over hydrogenation of furfural on Ru/Al-MIL-53	- The Al-MIL-53-BDC (ADP) were prepared by hydrothermal - The Al-MIL-53-BDC (ADP) were prepared by hydrothermal	-Liquid phase -Reduce at 200°C for 2h -Furfurl 100uL, temperature 20°C, catalyst 0.1 g, pressure 0.5MPa, water 9.9 mL	-The high activity is Ru/Al-MIL-53-BDC

Ref.	Purposes of study	Catalysts and preparation methods	Reaction conditions	Results
Yuan, Q. et al. (2015) [5]	Studied the Ru nanoparticles supported on a series of zirconium based metal organic frameworks for liquid phase hydrogenation of furfural	-The Ru catalysts were prepared by depositionreduction of Ru on the Zr-MOFs	-Liquid phase -Reduce at 200°C for 2h -Furfurl 100uL, catalyst 0.1 g, temperature 20°C, pressure 0.5MPa, water 9.9 mL	- Ru/UiO-66 showed the highest activity and reused in five reaction cycles without appreciable loss in performance.

Noble metals were investigated in the hydrogenation and it higher catalytic activity was found compared to the non-noble metal. Panagiotopoulou, P. et al. (2014) [31] studied in 2 researches, the first one was the methyl furan production by hydrogenation of furfural in the liquid phase on Ru/C catalyst. From the results, it is suggested that increasing of reaction temperature and/or reaction time enhance the yield of methylfuran. The Ru catalysts show significantly decrease of conversion when recycling experiments and furfuryl alcohol yield increases at the expense of methyl furan. Secondly, Panagiotopoulou, P. et al. studied the effect of alcohol hydrogen donor on methyl furan production by Ru/C catalyst [30]. Their results show the $Ru/RuO_2/C$ catalyst exhibits high performance of furfural conversion and selectivity to methyl furan because Ru on carbon support has high dispersion of metal particles on the support surface. The secondary alcohols showed the most effective in reaction which was coherent to Mironenko, R M. et al. (2015) [6] studied the formation and catalytic properties of the active sites in Pd/C and Ru/C catalysts for hydrogenation of furfural. It was found the highly active catalyst is Pd/C because the carbon support

affects to the dispersion of metal. The Ru catalyst showed low activity but high selectivity for furfuryl alcohol possibly due to irreversible adsorption of water on the active sites. From other methods of catalyst preparation, Yang, J. et al. (2016) [33] studied the effect of aromatic and aliphatic organic linkers over hydrogenation of furfural on Ru/Al-MIL-53. The framework containing an aromatic ring (Al-MIL-53-BDC) shows higher surface area than the analogue with an aliphatic linker (Al-MIL-53-ADP) which contributes to the Ru metal dispersion and enhanced substrate adsorption. And Yuan, Q. et al. (2015) [5] studied the Ru nanoparticles supported on a series of zirconium based metal organic frameworks for liquid phase hydrogenation of furfural. It was found the Ru/UiO-66 is the most efficient catalyst because the increased binding energy is caused by an increased dispersion of RuO_2 and interaction with the organic linkers of the MOF. It can be recycled in five consecutive reactions without appreciable loss in performance.

2.8 The bimetallic catalyst on furfural hydrogenation reaction

Table 2.5 Summary of the research on the bimetallic catalysts on furfural hydrogenation.

Ref.	Purposes of study	Catalysts and preparation methods	Reaction conditions	Results
Liu, L. et al. (2018) [1]	modified multiwalled carbon nanotubes via co-impregnation method for hydrogenation of furfural in liquid phase	-The bimetallic Pt-based and Pd-based were prepared by co-impregnation method	-Liquid phase -Reduce at 400°C for 4h -Furfurl 0.5mL, temperature 100°C, catalyst 0.1 g, pressure 3MPa, ethanol 5mL	-The Pt–Fe/MWNT and Pd–Ni/MWNT catalysts showed enhancing the catalytic activity for furfural hydrogenation

Ref.	Purposes of study	Catalysts and preparation methods	Reaction conditions	Results
Fulajtárova, K. et al. (2015) [33]	Studied the bimetallic Pd–Cu catalysts with different metals loadings on various supports for hydrogenation of furfural	-The Pd catalyst were prepared by impregnation method -The Pd-Cu/MgO catalyst were prepared by reduction with formaldehyde -The Pd-Cu/C were prepared using co-impregnation method and calcined at 250 °C for 5 h	-Liquid phase -Reduce at 300-450°C for 2h -Furfurl 0.6g, catalyst 0.1 g, temperature 110-130°C, time 8h, pressure 0.6-0.8MPa, water 10 mL	-The best catalytic performance exhibited catalysts prepared by electroless plating method -The high conversion and selectivity is 5%Pd–5%Cu/MgO catalyst
Zhang, C. et al. (2017) [4]	Synthesized the Silica-supported platinum overlayer on nickel or copper catalysts for furfural hydrogenation	The monometallic (Ni, Cu, and Pt) and bimetallic (Ni-Pt and Cu-Pt) were synthesized using incipient wetness impregnation of silica gel	-Liquid phase -Reduce at 400°C for 3h -Furfurl 5g, catalyst 0.1-0.3 g, temperature 250°C, time 10h, pressure 0.6-100psi, isopropanol 100g	-The Cu@Pt overlayer Catalyst showed high furfuryl alcohol selectivity

Ref.	Purposes of study	Catalysts and preparation methods	Reaction conditions	Results
Aldosari, O. F. et al. (2016) [7]	Studied the Pd–Ru/TiO2 catalyst and effect of the solvent for furfural hydrogenation	-The Pd, Ru, Pd-Ru on TiO2 were prepared by impregnation method andcalcined in static air (400 °C for 3 h	-Liquid phase -Reduce at 300°C for 2h -Furfurl 1g, catalyst 0.1 g, ambient temperature, time 2h, pressure 0.3MPa, solvent 15mL	-The 1% Ru : 4% Pd/TiO_2 is the best effective catalyst -The octane is the best solvent for selectivity
Musci, J. J. et al. (2017) [9]	Studied the carbon-supported Ru and RuSn catalysts for furfural hydrogenation	-The 3wt% Ru was prepared by impregnation on activated carbon -The RuSn were prepared by controlled surface reactions	-Liquid phase -Furfurl 0.45mL, catalyst 0.1 g, temperature 90°C, time 5h, pressure 1.25MPa, water 50mL	-The RuSn0.4/C catalyst achieved the high furfuryl alcohol selectivity -The Ru/C catalysts showed a high level of activity

The bimetallic catalyst on furfural hydrogenation reaction was studied and has shown resulted in the improving catalytic activity compared to monometallic catalysis. Liu, L. et al. (2018) [1] modified multi-walled carbon nanotubes via co-impregnation method for hydrogenation of furfural in liquid phase. From the results, it was found the Pt–Fe/MWNT showed the highest conversion and selectivity to furfuryl alcohol.

Pd–Ni/MWNT catalysts exhibited the best catalytic performance due to the effect of bimetallic catalysts improve catalytic activity and stability and attribute to active crystal planes exposed over Pt and Pd promoted by Fe and Ni. Fulajtárova, K. et al. (2015) [33] studied the bimetallic Pd–Cu catalysts with different metals loadings on various supports for hydrogenation of furfural. From the results, it was found the Pd–Cu catalysts supported on MgO and $Mg(OH)_2$ showed the highest conversion and selectivity to furfuryl alcohol because the Pd^0 sites and closely interacting bimetallic Pd^0–Cu_2O catalytic sites. The Cu^+ sites participate on activation of C=O group in furfural. The Cu promoted Pd was found to improve in conversion and selectivity to furfuryl alcohol. Zhang, C. et al. (2017) [4] synthesized the silica-supported platinum overlayer on nickel or copper catalysts for furfural hydrogenation and showed higher turnover frequencies of furfural hydrogenation compared to pure Pt and pure Cu. For the Cu@Pt, the Pt sites improve the efficiency of Cu catalyst by the blocking of Pt site perform by strong hydrogen adsorption, it decreased H_2 binding strength of Pt overlayer compared to pure Pt. Moreover, the Ru catalyst was interested in improving the selectivity to furfuryl alcohol. Aldosari, O. F. et al. (2016) [7] studied the Pd–Ru/TiO_2 catalyst and the effect of solvent for furfural hydrogenation. It was found that the octane solvent showed high activity and selectivity to 2-methylfuran and furfuryl alcohol as octane is a polar solvent. The effect of bimetallic by adding Ru particles to the Pd/TiO_2 showed the decreasing of conversion but improving the selectivity of 2-methylfuran and furfuryl alcohol and decreasing by product of reaction because Ru catalyst was highly selective catalyst to produce furfurly alcohol but it has low conversion for furfural hydrogenation. From the low conversion for furfural hydrogenation, the research for improved conversion was attempted by Musci, J. J. et al. (2017) [9]. The carbon-supported Ru and RuSn catalysts were investigated in furfural hydrogenation. It is suggested that the adding amount of tin to Ru catalyst improve the efficiency of catalyst for furfural hydrogenation, the Sn/Ru ratio of 0.4 promoted the C=O hydrogenation reaching a selectivity towards furfuryl alcohol because tin compromise between the dilution of Ru sites, active for the hydrogenation reaction but high concentration of tin did not improve the efficiency.

CHAPTER III

EXPERIMENTAL

3.1 Catalyst preparation

3.1.1 Preparation of TiO_2 sol-gel support

The TiO_2 sol-gel support was prepared by a sol-gel method. The titanium isopropoxide (TTIP) precursor containing 7.33 cm^3 of 65 vol. % nitric acid in 1000 cm^3 of deionized water was prepared under constant stirring. After adding 83.5 cm^3 TTIP into stirring mixture while precipitate was formed then the mixture was constantly stirred at room temperature for 3 days until the sol was clear. The clear sol was dialyzed in cellulose membrane in the deionized water for 3-4 days and the water was changed every day until the pH of water was 3.5. After that, the sol was dried in oven at 110°C overnight to taken off the solvent. The dried sol was milled and calcined by O_2 flow at 350°C for 2 h with heating rate of 10°C/min.[7]

Table 3.1 Chemical used for prepared TiO_2 by sol-gel method

Chemicals	Formula	Suppliers
Titanium isopropoxide	$Ti[OCH(CH_3)_2]_4$	Aldrich Chemical Ltd.
65% nitric acid	HNO_3	Asia Pacific Specialty Chemical Limited.

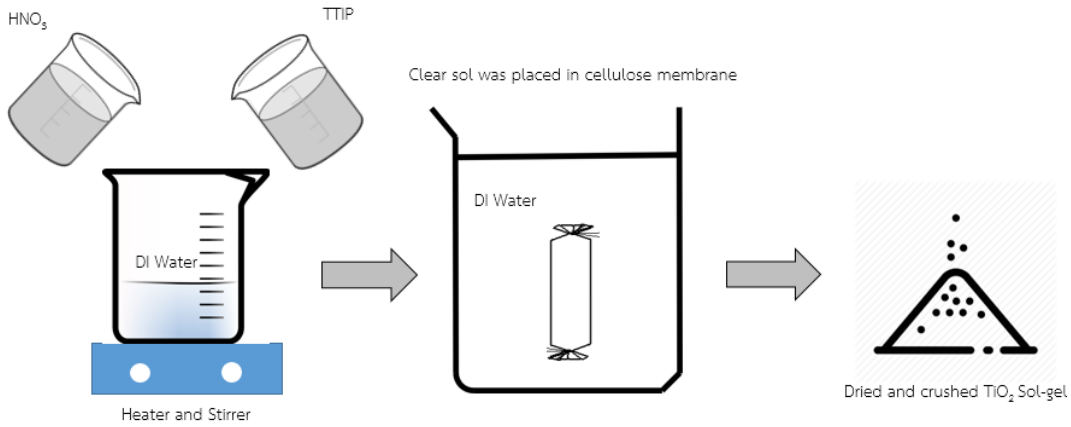

Figure 3.1 Diagram of TiO_2 catalysts preparation by sol-gel method

3.1.2 Preparation of SiO_2, TiO_2 (Rutile, P25, Anatase, Sol-gel) supported Ru and Co catalyst (monometallic)

The 1.5%wt Ru monometallic catalysts were prepared on various supports as shown in **Table 3.3.** The catalyst was prepared by incipient wetness impregnation method using ruthenium (III) nitrosylnitrate solution as the Ru precursor. The supports (TiO_2 with various phases: rutile, P25, anatase, and sol-gel and SiO_2 15nm) were impregnated with the Ru precursor solution until volume equals to pore volume of support. After that, the catalyst was left at room temperature for 6 h and dried by oven at 110°C for 12 h in air. The dried catalyst was calcined in air at 550°C for 4 h with heating rate 10°C/min. The 1.5%wt Co monometallic on TiO_2 anatase phase support was prepared by incipient wetness impregnation method followed the previously steps.

Table 3.2 Precursor used for incipient wetness impregnation method

Chemicals	Formula	Suppliers
Ruthenium (III) nitrosylnitrate solution	$Ru(NO)(NO_3)_x(OH)_y$, x+y=3	Aldrich Chemical Ltd
Cobalt naphthenate solution	$CoC_{22}H_{14}O_4$	Aldrich Chemical Ltd

Table 3.3 Support used for incipient wetness impregnation method

Chemicals	Formula	Suppliers
Rutile	TiO_2	Aldrich Chemical Ltd
P25	TiO_2	DEGUSSA
Anatase	TiO_2	Alfa Aesar
Sol-gel	$Ti[OCH(CH_3)_2]_4$	Aldrich Chemical Ltd
SiO_2	SiO_2	Aldrich Chemical Ltd

3.1.3 Preparation of TiO_2 (Anatase) supported Ru-Co catalyst (bimetallic)

The 1.5%wt Ru with various contents of Co bimetallic catalysts on TiO_2 anatase phase supports were prepared by incipient wetness impregnation method using ruthenium (III) nitrosylnitrate solution and cobalt naphthenate solution as Ru precursor and Co precursor, respectively. The TiO_2 anatase phase support was impregnated with the mixture of Ru precursor solution and Co precursor solution until volume equals to pore volume of support. After that, the catalyst was left at room temperature for 6 h and dried by oven at 110°C for 12 h in air. The dried catalyst was calcined in air at 550°C for 4 h with heating rate 10°C/min.

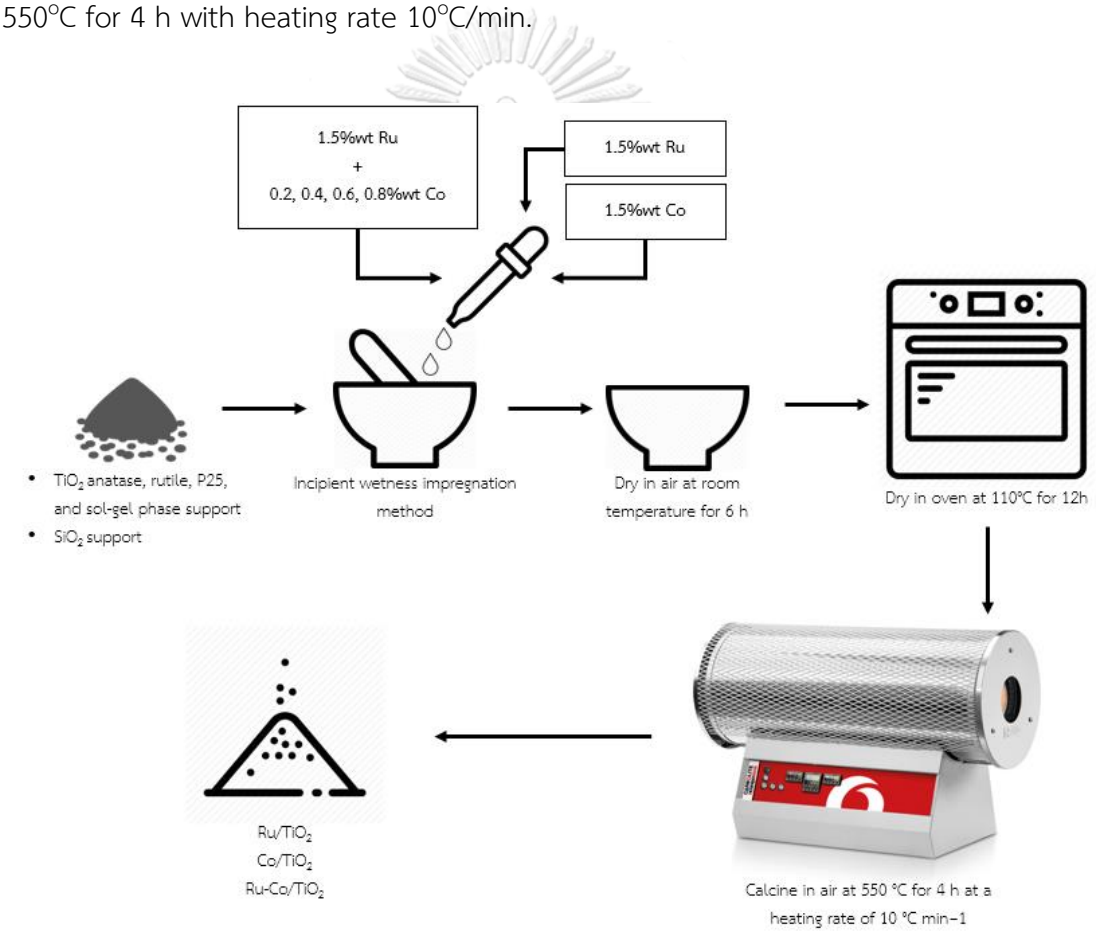

Figure 3.2 Diagram of Ru, Co, Ru-Co on TiO_2 catalysts preparation by incipient wetness impregnation method

3.2 Catalyst pretreatment

Before hydrogenation reaction, the catalyst was pretreated by reduction technique to make the catalyst in reduced form. Quartz wool was contained into the glass u-tube cell and 0.06g of catalyst was loaded into the glass u-tube cell. The catalyst was reduced in a MicromeriticsChemiSorb 2750 with a H_2 flow 25cm^3/min at 300°C for 2h. After that, the catalyst was cooled down with a N_2 flow 25cm^3/min from 300°C to 30°C.

3.3 Catalyst test in the furfural hydrogenation

The furfural hydrogenation was carried out in a liquid-phase in order to investigate the catalytic performances. 0.05g of reduced catalyst, 10ml of methanol and 50µl of furfural were loaded into the 100 ml stainless steel autoclave reactor (JASCO, Tokyo, Japan) supplied with hot plate and magnetic stirrer and then set temperature to 50°C by heating in a water bath. After that, the autoclave reactor was purged with H_2 for 3 times. The furfural hydrogenation reaction was carried out at 20bar of H_2 at 50°C for 2h and the reaction mixture was stirred with magnetic stirrer at 900 rpm to eliminate the external mass transfer resistance. When the reaction was done, the stirrer was stopped and the autoclave reactor was cooled down to 20°C by ice-water. The reaction mixture was centrifuged and separated from the catalyst. The liquid product was analyzed by a gas chromatography equipped with a flame ionization detector (FID).

Table 3.4 Chemicals used in the liquid-phase furfural hydrogenation

Chemicals	Formula	Suppliers
Furfural 99%	$C_5H_4O_2$	Aldrich
Furfuryl alcohol 99%	$C_5H_6O_2$	Aldrich
Tetrahydrofurfuryl alcohol 98%	$C_5H_{10}O_2$	Aldrich
Furan 98%	C_4H_4O	Aldrich
Methanol 98%	CH_3OH	Aldrich

Table 3.5 The operating conditions of gas chromatograph with a flame ionization detector

Gas chromatograph	**Shimadzu GC-2014**
Detector	FID
Capillary column	Rtx®5
Carrier gas	Helium (99.99 vol. %)
Make-up gas	Air (99.9 vol. %)
Column temperature	110°C
Injector temperature	260°C
Detector temperature	270°C
Time analysis	41.80 min

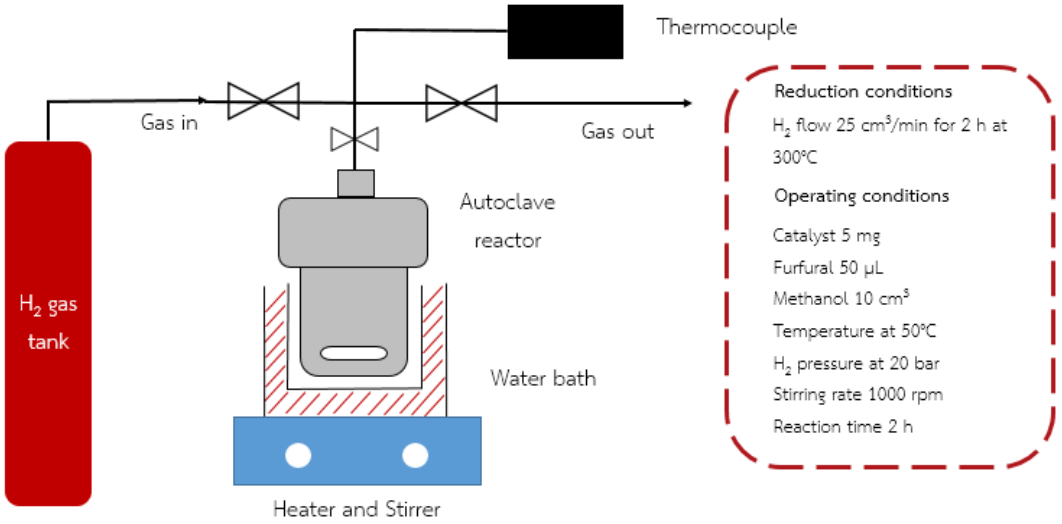

Figure 3.3 The liquid-phase of furfural hydrogenation

3.4 Catalyst Characterization

3.4.1 X-ray diffraction (XRD)

The XRD patterns and crystalline size of the catalysts were studied by The X-ray diffraction technique on a SIEMENS D5000 X-ray diffractometer with CuKα radiation in scanning range from 20° to 80° 2θ.

3.4.2BET surface area

The BET specific surface area, pore volumes, hyteresis loop, and pore size diameters of the catalysts were investigated by the N_2 physisorption technique on a Micromeritics ASAP 2020 automated system.

3.4.3 Hydrogen Temperature-programmed reduction (H_2-TPR)

The reducibility of catalysts and the interaction of metal and support were demonstrated by temperature programmed reduction technique on a MicromeriticsChemiSorb 2750 with ChemiSoftTPx software. The Removing adsorbed method, 0.1g of catalysts were packed in a quartz U-tube and pretreated with a N_2 flow 25cm^3/min at 200°C for 1h and then cooled down to the room temperature. Following this the gas flow was changed to 10%H_2/Ar and temperature was ramped to 800°C by ramped rate 10°C min^{-1} with a 30min hold at 800°C

3.4.4 X-ray photoelectron spectroscopy (XPS)

The binding energy of catalysts were characterized using a Kratos AMICUS X-ray photoelectron spectroscopy operated with an Mg Kα X-ray as primary excitation and KRATOS VISION II software. The XPS spectra of C1s peak was specified as reference at binding energy of 285.0eV.

3.4.5 Co-pulse Chemisorption (CO-Chem)

The amounts of CO chemisorbed on the catalyst, metal active sites, and percentages dispersion of metal were defined by The CO-pulse chemisorption technique on a MicromeriticsChemiSorb 2750 with ChemiSoftTPx software. The 0.05g of catalysts were packed in a quartz U-tube cell and introduced with a He flow 25cm^3/min to take out of air and then catalyst was reduced with H_2 flow 25 cm^3/min and heated from 30°C to 300°C for 2h with a heating rate of 10°C/min. After catalyst was cooled down to 30°C in a He flow and injected with CO into the cell by pulse method for adsorb on the active sites of catalyst while unabsorbed CO was detected by the thermal conductivity detector. The injecting of CO was stopped until the unabsorbed CO peaks were constant.

3.4.6 Transmission electron microscopy (TEM)

The particles size of metal and the morphology of catalysts were carried out using JEOL-JEM 2010 transmission electron microscope using energy-dispersive X-ray detector operated at 200kV.

3.4.7Scanning electron microscopy and energy dispersive X-ray spectroscopy (SEM-EDX)

The element distribution and percent metal on the catalyst were characterized by JEOL mode JSM-6400 Scanning electron microscope and Link Isis Series 300 program energy dispersive X-ray spectroscopy. The samples were pretreated at 110°C for 24h before analysis.

CHAPTER IV

RESEARCH METHODOLOGY AND REDEARCH PLAN

4.1 The research methodology

The research methodology consists of two parts.

Part I. Part I. The investigation of the characteristics and catalytic properties of TiO_2 supported Ru nanoparticles prepared with different phases of TiO_2 in the liquid-phase furfural hydrogenation.

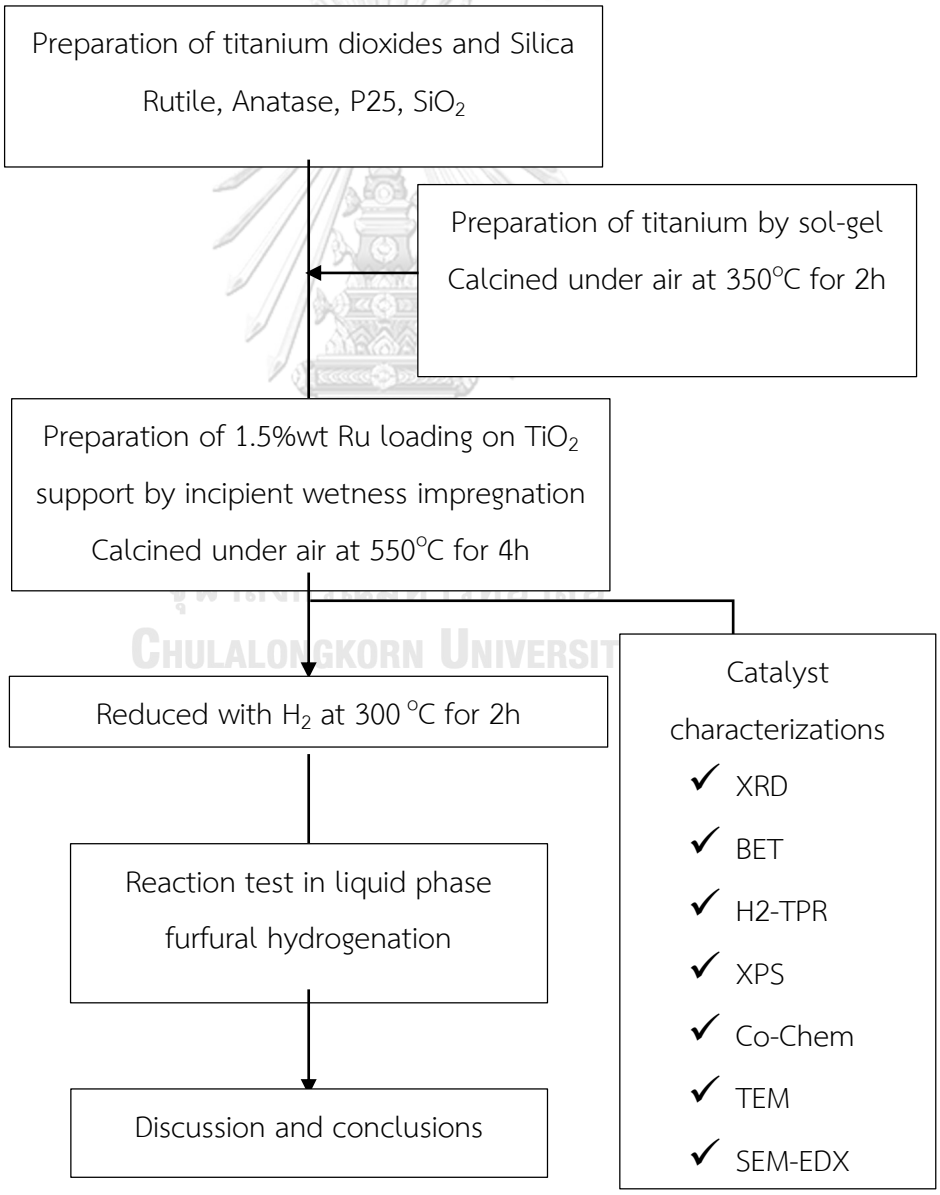

Part II. Study of the effect of bimetallic Ru-Co nanoparticles supported on TiO_2 anatase phase catalyst in liquid-phase furfural hydrogenation.

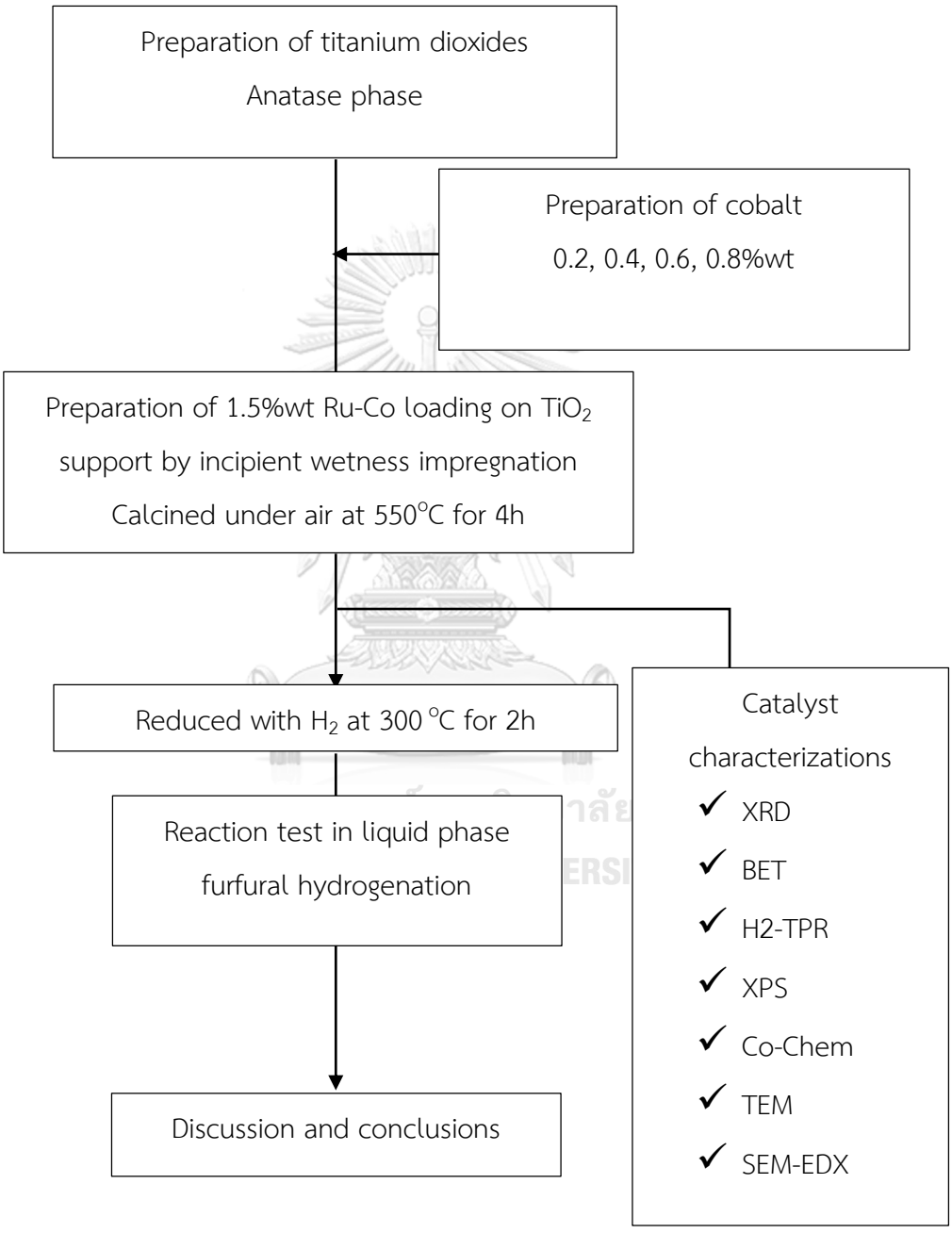

CHAPTER V
RESULTS AND DISSCUSSION

The results and discussion of the characteristics and catalytic properties of the monometallic Ru/TiO_2 and bimetallic Ru-Co/TiO_2 catalysts in the liquid phase of furfural hydrogenation are divided into two parts. In the first part, the investigation of the characteristics and catalytic properties of TiO_2 supported Ru nanoparticles prepared with different phases of TiO_2 in the liquid-phase furfural hydrogenation was reported. The TiO_2 supported Ru nanoparticles with different phases of TiO_2 prepared by the incipient wetness impregnation method were analyzed by XRD, N_2-physisorption, H_2-temperature programmed reduction (H_2-TPR), X-ray photoelectron spectroscopy (XPS), CO-pulse Chemisorption, Scanning electron microscopy and energy dispersive X-ray spectroscopy (SEM-EDX). In the second part, the effect of bimetallic Ru-Co nanoparticles supported on anatase phase TiO_2 catalysts in the liquid-phase furfural hydrogenation was discussed. The characteristics and catalytic properties of Ru (1.5wt% Ru) and Co (0.2, 0.4, 0.6, and 0.8wt% Co) on TiO_2 anatase phase prepared by the incipient wetness impregnation method were analyzed by XRD, N_2-physisorption, H_2-TPR, XPS, CO-pulse chemisorption, SEM, and TEM.

Part I. The investigation of the characteristics and catalytic properties of TiO_2 supported Ru nanoparticles prepared with different phases of TiO_2 in the liquid-phase furfural hydrogenation.

5.1 Characterization of Ru/TiO_2 with different TiO_2 phases and Ru/SiO_2

5.1.2 N_2 Physisorption

The N_2 adsorption-desorption isotherms, pore structure, BET surface area, pore volume, pore size, and the average anatase Ru/TiO_2 crystallite size of Ru/TiO_2 with different phases of TiO_2 and SiO_2 catalysts were measured by the Brunauer Emmett Teller (BET) method and the results are shown in **Table 5.2.** From the results, there were no significant differences in BET surface area, pore volume and pore size of Ru/TiO_2-A, Ru/TiO_2-P25, and Ru/SiO_2. The Ru/TiO_2-Sol showed high BET surface area at 106 m^2/g. However, the heat treatment brings the disadvantage of the aggregation of TiO_2 particles [34] and small pore size at 5 nm. The pore structure of Ru/TiO_2-Sol synthesized by sol-gel method depended on the desired pore size of the membrane [35]. The particle size and homogeneity in particle distribution can be controlled by Sol-gel technique. Moreover, the hole-structure was collapsed due to the surface tension of the solvents [34]. The Ru/TiO_2-R had high BET surface area at 144 m^2/g and large pore volume at 0.83 cm^3/g that was proved by hysteresis loop of Ru/TiO_2-R in **Figure 5.3**. The average anatase TiO_2 crystallite size of Ru/TiO_2-A, Ru/TiO_2-P25 catalysts were not significant different at around 28 nm but was smaller for the Ru/TiO_2-R at 17 nm. However, Ru/TiO_2-Sol exhibited the smallest crystallite size due to the preparation by sol-gel technique [34].

The N_2 adsorption-desorption isotherms of Ru/TiO_2-A, Ru/TiO_2-P25, Ru/TiO_2-R, Ru/TiO_2-Sol, and Ru/SiO_2 are shown in **Figure 5.3.** From Brunauer-Deming-Teller (BDTT), the isotherms of Ru/TiO_2-A, Ru/TiO_2-P25, Ru/TiO_2-R, Ru/TiO_2-Sol, and Ru/SiO_2 were type-IV physisorption isotherm, showing the characteristic of mesoporous materials with pore diameters between 2 and 50 nm. The shape characteristic of hysteresis loop for all the catalysts except Ru/TiO_2-Sol were type H3 indicating to the

slit-like pore. The Ru/TiO_2-Sol showed type H1 hysteresis loop which described a narrow distribution of relatively uniform pores.

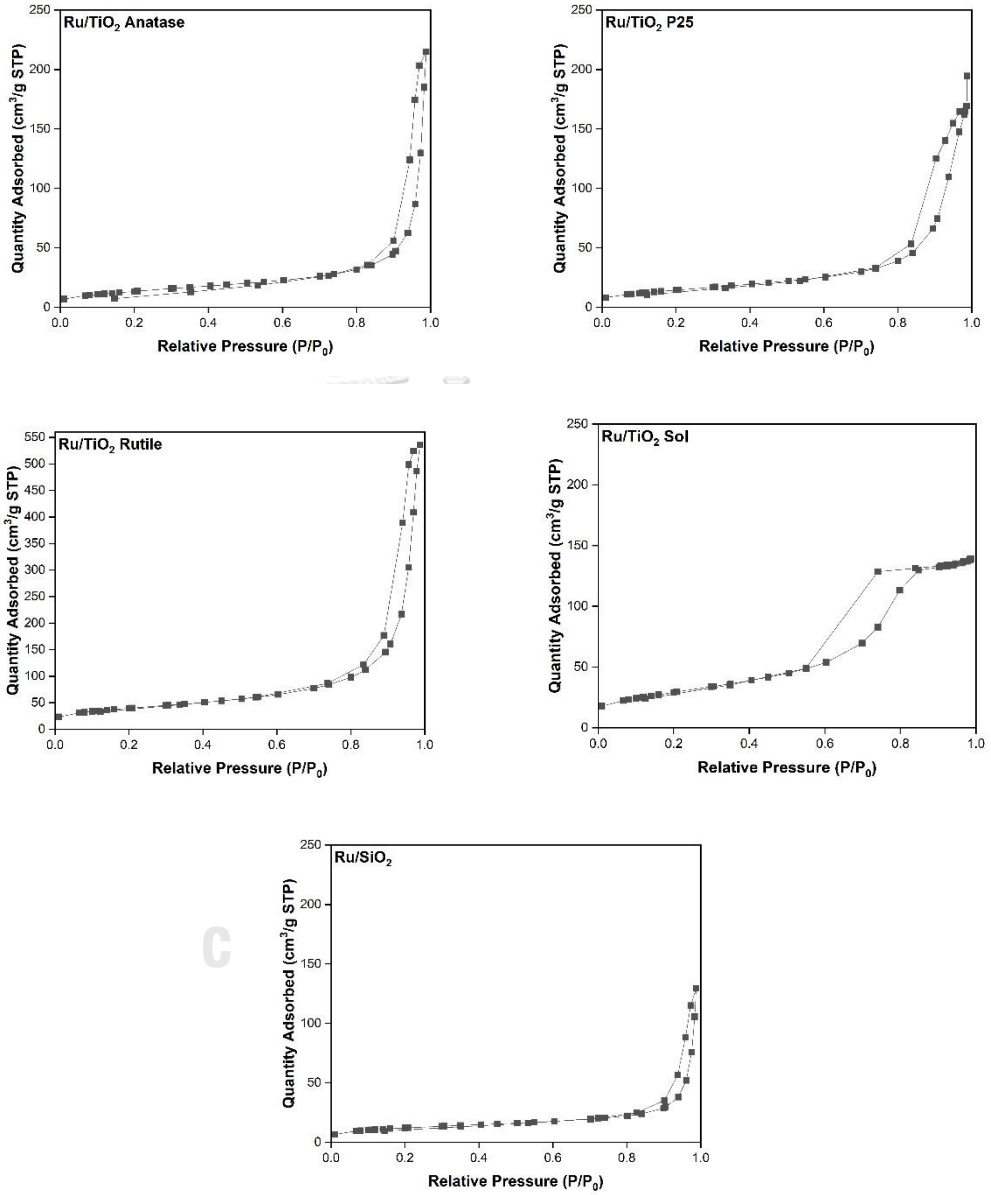

Figure 5.1 N_2-Physisorption isotherms of Ru/TiO_2-A, Ru/TiO_2-P25, Ru/TiO_2-R, Ru/TiO_2-Sol, and Ru/SiO_2

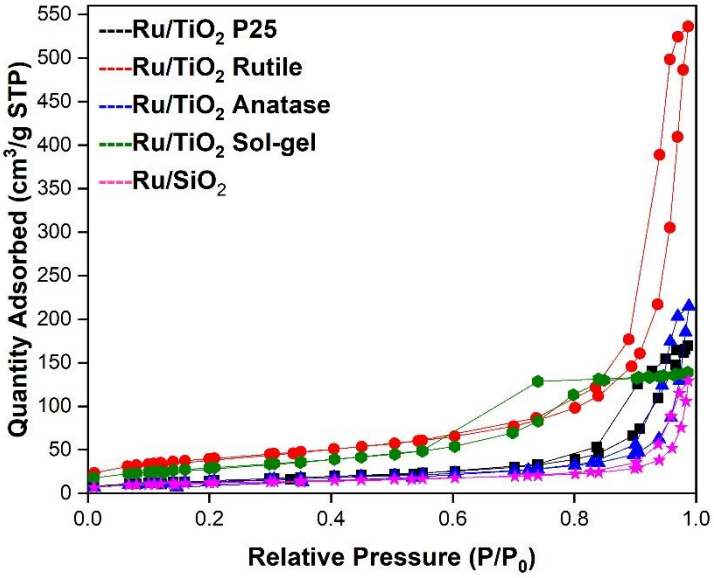

Figure 5.2 The combination of N_2-Physisorption isotherms of Ru/TiO_2-A, Ru/TiO_2-P25, Ru/TiO_2-R, Ru/TiO_2-Sol, and Ru/SiO_2

Table 5.1 Physical properties of the Ru/TiO_2 with different phases of titania and Ru/SiO_2 catalysts.

Sample	Avg. crystallite size[a] of anatase TiO_2 (nm)	BET surface area (m^2/g)	Pore volume[b] (cm^3/g)	Avg Pore size[b] (nm)
Ru/TiO_2-A	27.9[c]	50	0.32	22.0
Ru/TiO_2-R	16.9[d]	144	0.83	18.5
Ru/TiO_2-P25	27.9[c]	53	0.26	15.5
Ru/TiO_2-Sol	8.6[c]	106	0.21	5.0
Ru/SiO_2	-	44	0.20	18.2

[a]Based on the XRD results.

[b]Determined from the Barret-Joyner-Halenda (BJH) desorption method.

[c] Determined from anatase peak at 25° 2θ

[d] Determined from rutile peak at 27° 2θ

5.1.3 H_2-temperature programmed reduction

Temperature programmed reduction was employed to determine the reducibility, reduction behaviors of Ru/TiO_2 with different TiO_2 phases catalysts, as well as to obtain the information regarding the interaction between the metal and support. The reduction behaviors of Ru/TiO_2 Anatase, Ru/TiO_2 Rutile, Ru/TiO_2 Sol-gel, Ru/TiO_2 P25 catalysts are shown in **Figure 5.5**. From the results, all the Ru/TiO_2 showed three main reduction peaks at about 140℃ - 200℃ as a result of the reduction of Ru(III) to Ru(0) and at 320℃ - 410℃ as a result of Ru interacted with TiO_2 support [36] and Ru-TiOx species interacted with TiO_2 support [37]. The last board peak at 570℃ - 720℃, which can be assigned to the reduction of surface TiO_2 [38]. The Ru reduction peak of Ru/TIO_2-A and Ru/TiO_2-Sol showed a single sharp peak, suggesting that the Ru particles on Anatase and Sol-gel phase of TiO_2 were homogeneity in particle size distribution [34]. However, the Ru reduction peak of Ru/TIO_2-P25 and Ru/TiO_2-R displayed a series of convoluted peaks probably due to the presence of Ru with different particles sizes and/or presence of Ru ions in different environments on the surface of the support [39].

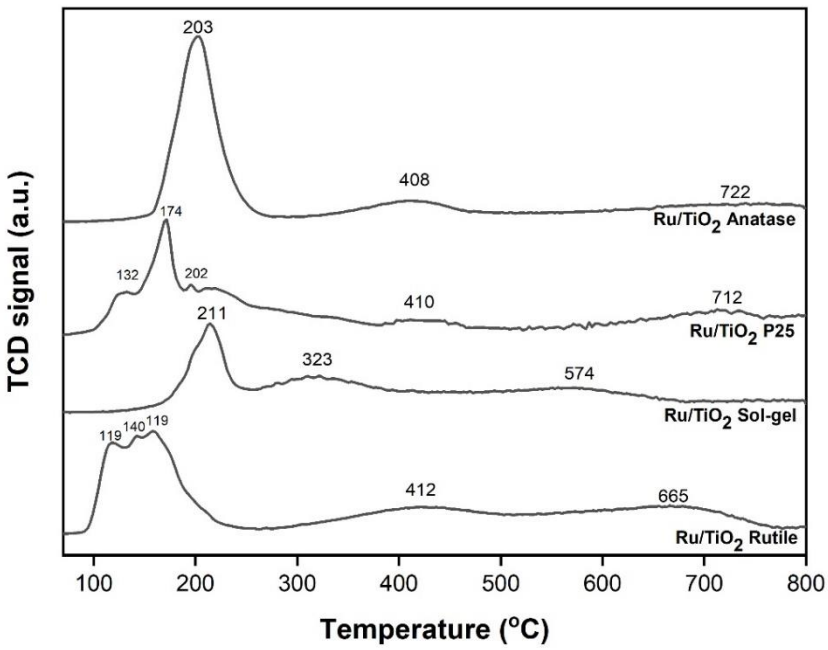

Figure 5.3 The H_2-TPR profiles of Ru/TiO_2 Anatase, Ru/TiO_2 Rutile, Ru/TiO_2 Sol-gel, Ru/TiO_2 P25 catalysts

Table 5.2 H_2 consumption of Ru-TiO_x peak with different phase of TiO_2 catalysts

Catalysts	H_2 consumption of Ru-TiO_x interface species interacting with support (mmol/g)
Ru/TiO_2-A	2.72
Ru/TiO_2-R	3.12
Ru/TiO_2-P25	1.94
Ru/TiO_2-Sol	2.33

According to the H_2-TPR results, the Ru reduction peak of Ru/TiO_2-A was observed at 203°C and the Ru interacted with TiO_2 support peak was shown at 408°C. The Ru reduction peak of Ru/TiO_2-P25 and Ru/TiO_2-R appeared at low temperature around at 174°C and 140°C, respectively because the size of Ru particles of Ru/TiO_2-P25 and Ru/TiO_2-R were smaller than Ru/TiO_2-A [39]. However, the Ru interacted with TiO_2 support peak of both catalysts were not significant different. From the H_2-TPR results, smaller Ru particles size usually exhibited Ru reduction peak at lower temperature. Therefore, increasing of Ru particles size resulted in a shift of Ru reduction peak to higher temperature [39-41]. The last board peaks of Ru/TiO_2-A, Ru/TiO_2-P25, and Ru/TiO_2-R were varied between 665°C and 772°C. However, the Ru/TiO_2-Sol showed the peak of Ru reduction at 211°C which was higher than Ru/TiO_2-P25, suggesting that the Ru particles of Ru/TiO_2-Sol were smaller than Ru/TiO_2-P25 but the Ru interacted with TiO_2 support peak and the reduction of TiO_2 surface showed the lowest temperature among all the catalysts at 323°C and 574°C, respectively because of the weak interaction between Ru metal and TiO_2-Sol support [41]. The H_2 consumption of Ru-TiO_x species is given in **Table 5.2** and was found to be in the order Ru/TiO_2-R > Ru/TiO_2-A > Ru/TiO_2-Sol > Ru/TiO_2-P25.

5.1.1 X-ray diffraction (XRD)

The structure, crystallization and phase composition of TiO_2 catalysts were analyzed by X-ray diffraction technique. The XRD patterns of the catalyst samples were measured from 20° to 80° 2θ. In Figure 5.1, the XRD characteristic peaks

showed anatase phase at 2θ = 25° (major), 37°, 48°, 55°, 56°, 62°, 71°, 75° and rutile phase at 27° (major), 36°, 42°, and 57° without formation of brookite phase, The diffraction peaks of Ru species were not observed in all the catalysts because of low content of Ru loading [42]. The average crystallite size of anatase and rutile phase TiO_2 in different supports were calculated by Scherrer's equation from the full width at half maximum of the XRD peak at 2θ = 25° (major) of anatase phase and 2θ = 27° (major) of rutile phase.

The XRD analysis of Ru/SiO_2 are shown in Figure 5.2, the wide angle XRD reveals the presence of a broad peak at 2θ = 22° which is because the amorphous SiO_2 support but no diffraction peaks for Ru were detected for catalyst. This is due to low amount Ru metal loading [43].

The amount of Anatase phase was calculated using the areas of the major anatase at 2θ = 25° and rutile 2θ = 27° of XRD peaks following the method described by Jung et al [44]. In Table 5.1, The Ru/TiO_2 catalysts consisting of 97, 87, 75, and 5% Anatase phase were called as Ru/TiO_2-A, Ru/TiO_2-P25, Ru/TiO_2-Sol, and Ru/TiO_2-R, respectively.

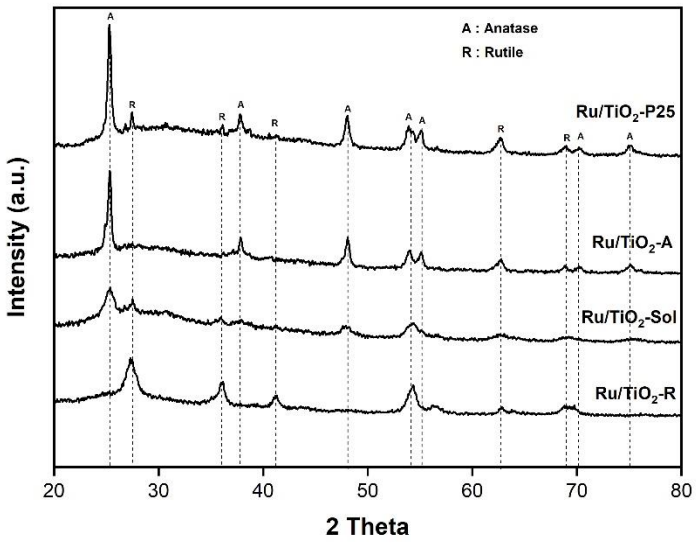

Figure 5.4 The XRD patterns of Ru/TiO_2 catalysts prepared with different TiO_2 phases

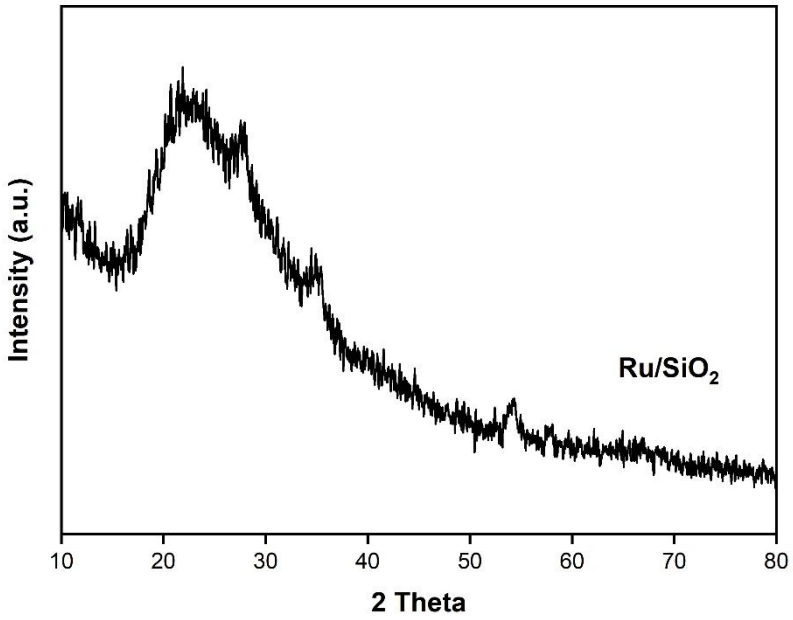

Figure 5.5 The XRD patterns of Ru/SiO_2 catalysts

Table 5.3 Ru/TiO_2 prepared with different phases of TiO_2 samples consisting of various % anatase of TiO_2

Sample	Anatase phase[a, b] (%)	Rutile phase[a, b] (%)
Ru/TiO_2-A	97	3
Ru/TiO_2-R	5	95
Ru/TiO_2-P25	87	13
Ru/TiO_2-Sol	75	25

[a]Based on the XRD results.

[b]Determined from a method described in Jung et al.

5.1.4 CO-pulse Chemisorption

The amounts of CO chemisorption on Ru/TiO_2 with different phases of TiO_2 catalysts after reduced at 300°C and the amount of Ru active sites were determined by the chemisorption based on the assumption CO : RU = 1 : 1 and the results are shown in **Table5.4**. The %Ru dispersion on Ru/TiO_2-R, Ru/TiO_2-P25, Ru/TiO_2-Sol, and

Ru/TiO_2-A were 5.0%, 4.6%, 2.2%, and 1.5%, respectively. It was found that Ru dispersion on TiO_2-P25 and Ru/TiO_2-R were similar and higher than Ru/TiO_2-Sol, and Ru/TiO_2-A. Moreover, the dispersion of Ru on TiO_2-A was the lowest. Similar has been found by Niu et al. [40] that anatase phase TiO_2 led to poor Ru dispersion. The size of Ru particles were also affected by the dispersion of Ru on TiO_2 support. According to Elzbieta, T. et al. (2017) [45], increasing of Ru particle size decreased the dispersion of Ru on TiO_2 support.

Table 5.4 CO chemisorption and metal concentrations of Ru/TiO_2 with different phase of TiO_2 catalysts

Catalysts	**Co chemisorption (Molecule Co × 10^{17}/g cat.)**	**Ru dispersion[a, b] (%)**
Ru/TiO_2-A	13.4	1.5
Ru/TiO_2-R	44.7	5.0
Ru/TiO_2-P25	41.1	4.6
Ru/TiO_2-Sol	19.7	2.2

[a] Determined from 1.5% of Ru

[b] Determined from CO-pulse chemisorption technique with the chemisorption based on the assumption CO : Ru = 1 : 1

5.1.5 Scanning electron microscopy and energy dispersive X-ray spectroscopy (SEM-EDX)

The morphology, element distribution, and percent metal on the catalyst were analyzed by SEM-EDX. In **Figure 5.6**, the SEM images of the Ru/TiO_2-A, Ru/TiO_2-R, and Ru/TiO_2-Sol catalysts showed similar morphology and characteristic shape but the Ru/TiO_2-Sol catalyst was constituted of aggregation of small grains [46]. Elemental analysis by EDX indicated that the chemical compositions were close to stoichiometrical percantages of Ru around 1.5wt% for all the catalysts.

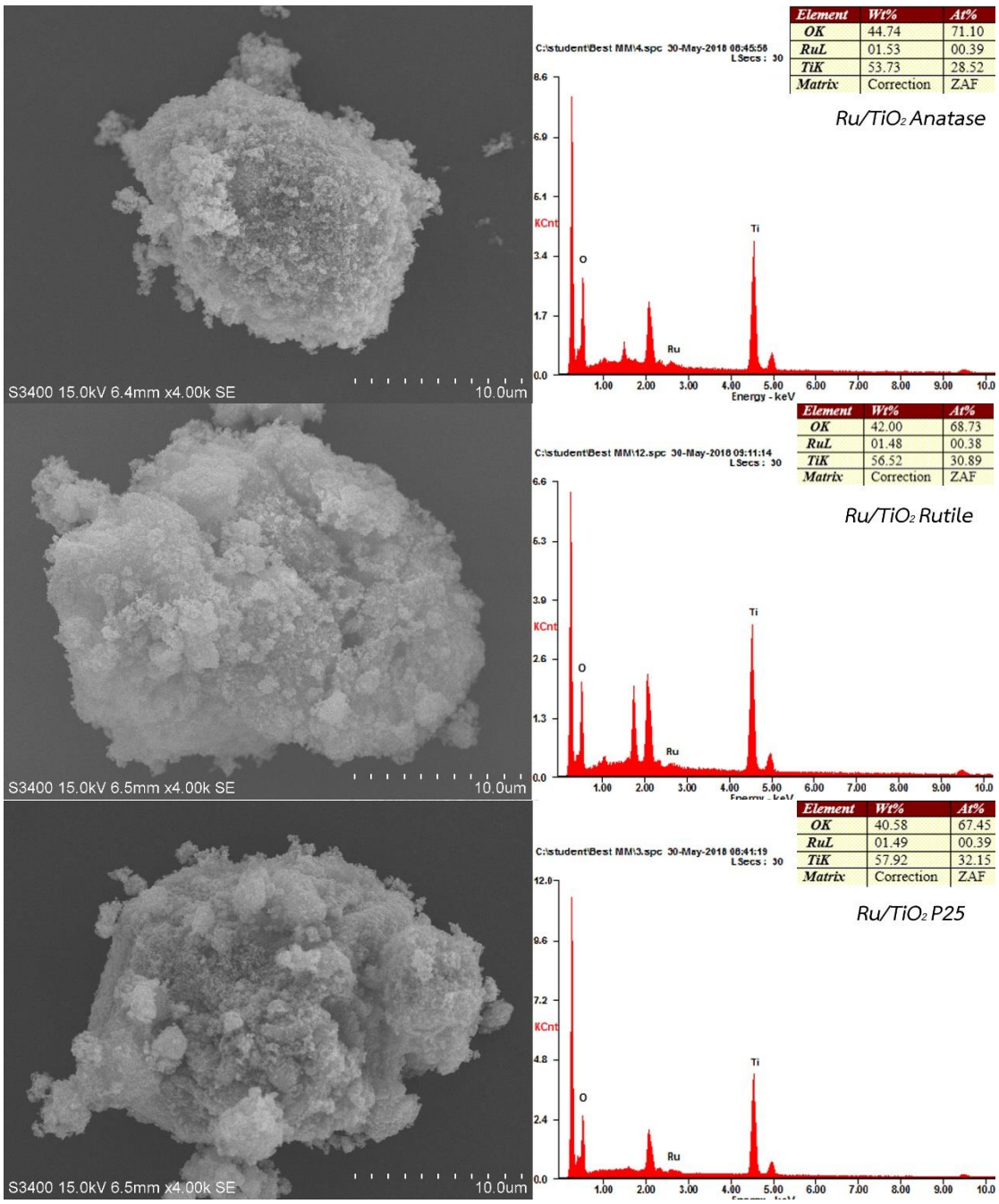
S3400 15.0kV 6.4mm x4.00k SE
10.0um
C:\student\Best MM\4.spc 30-May-2018 08:45:58
LSecs : 30
KCnt
O
Ti
Ru
Energy - keV
Element | Wt% | At%
OK | 44.74 | 71.10
RuL | 01.53 | 00.39
TiK | 53.73 | 28.52
Matrix | Correction | ZAF
Ru/TiO2 Anatase
S3400 15.0kV 6.5mm x4.00k SE
10.0um
C:\student\Best MM\12.spc 30-May-2018 09:11:14
LSecs : 30
KCnt
O
Ti
Ru
Element | Wt% | At%
OK | 42.00 | 68.73
RuL | 01.48 | 00.38
TiK | 56.52 | 30.89
Matrix | Correction | ZAF
Ru/TiO2 Rutile
S3400 15.0kV 6.5mm x4.00k SE
10.0um
C:\student\Best MM\3.spc 30-May-2018 08:41:19
LSecs : 30
KCnt
O
Ti
Ru
Element | Wt% | At%
OK | 40.58 | 67.45
RuL | 01.49 | 00.39
TiK | 57.92 | 32.15
Matrix | Correction | ZAF
Ru/TiO2 P25

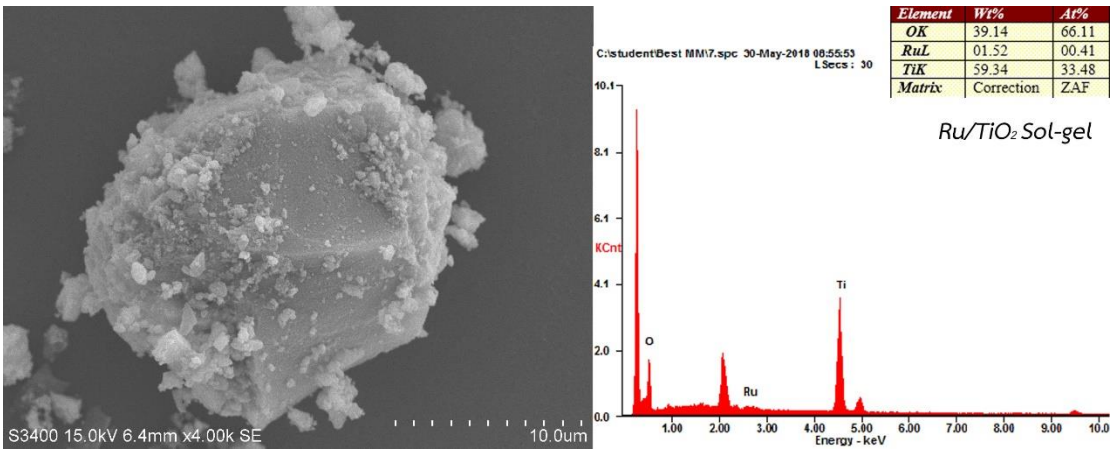

Figure 5.6 The SEM-EDX of Ru/TiO_2 Anatase, Ru/TiO_2 Rutile, Ru/TiO_2 Sol-gel, Ru/TiO_2 P25 catalysts

5.2 Activity test in the liquid-phase furfural hydrogenation

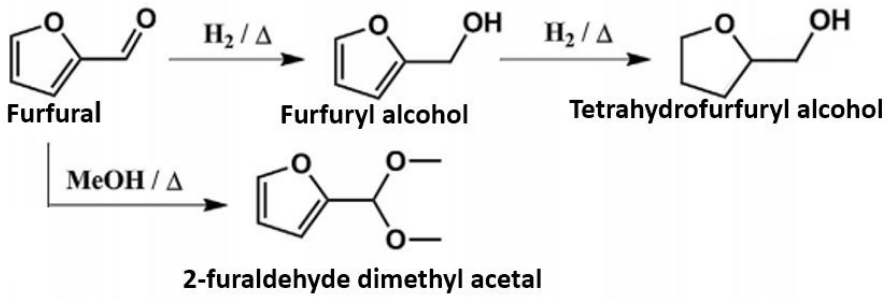

Figure 5.7 The pathway of furfural hydrogenation reaction [47]

The furfural hydrogenation reaction as shown in **Figure 5.7**, exhibited the 2 main reaction pathways. The first pathway is the hydrogenation in 2 steps of the C=O double bond that converts furfural to furfuryl alcohol and the further hydrogenation of the C=C double bond producing tetrahydrofurfuryl alcohol. The second pathway is the hydrogenation of C=O double bond with methanol, which converts furfural to 2-furaldehyde dimethyl acetal, which is the side-product of reaction between furfural and alcohol solvent. In contrast, non-polar solvents conferred poor furfural conversion, while methanol favored acetal by-product formatiol [47]. Taylor, M. et al. (2016) [47] studied the side effect from selective hydrogenation of furfural over supported Pt nanoparticles under mild conditions and showed that the selectivity

towards the undesired acetal side product decreased from ethanol>methanol>n-butanol. In the methanol case small amounts of 2-furaldehyde dimethyl acetal was found after 7h reaction. In our study of furfural hydrogenation reaction, furfuryl alcohol is the desired product and tetrahydrofurfuryl alcohol and 2-furaldehyde dimethyl acetal are the undesired products.

The catalytic performances of 1.5%Ru/TiO_2 prepared with different phases of TiO_2 catalysts were investigated in the selective hydrogenation of furfural in methanol solvent at temperature 50°C at a H_2 pressure of 2 bar and 2h reaction time. The catalytic behaviors of the Ru/TiO_2 with different phases of TiO_2 catalysts including furfural conversion and product selectivity are reported in **Table 5.5**, the main product was furfuryl alcohol and the by-product was 2-furaldehyde dimethyl acetal. The main product furfuryl alcohol was not hydrogenated to tetrahydrofurfuryl alcohol probably due to the time of reaction not long enough and/or the characteristics of the Ru/TiO_2 catalysts [48]. On the other hand, the by-product 2-furaldehyde dimethyl acetal was found in small amount. It was found that the Ru/TiO_2 catalysts were very selective to furfuryl alcohol. The Ru/SiO_2 catalysts showed very low conversion of furfural therefore it was not interesting in this research. The Ru/TiO_2-A catalyst exhibited the highest catalytic activity among all the catalysts, which could be attributed to the percentages of anatase phase as shown in **Table 5.1.** The catalytic activity decreased with the decreasing of the percentages of anatase phase. This result suggested the percentages of anatase in TiO_2 were the important factor attributing to the catalytic activity of Ru catalyst in the hydrogenation reaction of furfural to furfuryl alcohol. From **Table 5.1**. The percentages of anatase of Ru/TiO_2-A, Ru/TiO_2-P25, Ru/TiO_2-Sol, and Ru/TiO_2-R were calculated to be 97%, 87%, 75%, and 5%, respectively the percentage of anatase was found be the main important factor affecting the catalytic activity, the anatase phase TiO_2 is stable in nanometer-siged and hydrogen can pass through the anatase phase of TiO_2 surface and can be incorporated and store into anatase phase of TiO_2 where it leads to a significant band gap reduction. In other words, the anatase phase of TiO_2 are favorable adsorption sites for hydrogen atoms [49, 50]. For the rutile phase TiO_2, the catalytic activity and selectivity of furfuryl alcohol were diminished

because molecular hydrogen could not be interacted strongly with the rutile phase TiO_2, while atomic hydrogen readily sticks to the surface oxygen atoms [49].

The Ru/TiO_2-Sol displayed the selectivity of furfuryl alcohol was the lowest. This may be because of the weak interaction of Ru and TiO_2 support peak of H_2-TPR that was shifted to low temperature. However, the interaction of Ru and TiO_2 support peak of Ru/TiO_2-A, Ru/TiO_2-R, and Ru/TiO_2-P25 were equal position but the H_2 consumption of Ru-TiOx interface species were different. The selectivity of furfuryl alcohol was decreased by the decreasing of H_2 consumption of Ru-TiOx interface species as shown in **Table 5.3** because the lone pair electron of C=O are favorable Ru-TiOx interface species [37, 51]. The CO chemisorption results and the N_2 Physisorption results could not described the catalytic activity in this reaction. Different crystalline TiO_2 as supports for Ru nanoparticles was found to have a marked impact on the catalytic performances. Thus, the main factors to improve the catalytic activity in terms conversion are the percentage of anatase in the TiO_2 support and selectivity are the H_2 consumption of Ru-TiOx interface species interacting with support.

Table 5.5 Conversion of furfural and selectivity to furfuryl alcohol of Ru/TiO_2 with different phase of TiO_2

Catalysts	Conversion (%)	Selectivity to FA[a]	Selectivity to SP[b]
Ru/TiO_2-A	31.8	90.0	10.0
Ru/TiO_2-P25	20.0	85.3	14.7
Ru/TiO_2-Sol	17.5	75.1	24.9
Ru/TiO_2-R	4.4	96.3	5.7
Ru/SiO_2	10.0	85.4	14.6

Reaction (50μL furfural in 10 ml methanol) at 50°C under 20 bay H_2 with a 50 mg catalyst in 120 min

[a] Selectivity of furfuryl alcohol

[b] Selectivity of 2-furaldehyde dimethyl acetal

Part II. Study of the effect of bimetallic Ru-Co nanoparticles supported on TiO_2 anatase phase catalyst in liquid-phase furfural hydrogenation.

5.3 Characterization of Ru-Co/TiO_2 with different Co contents

5.3.1 X-ray diffraction (XRD)

In **Figure5.8** shows the XRD patterns of Ru-Co/TiO_2 catalysts with different Co contents prepared by the incipient wetness impregnation method. The Co content was varied at 0.2, 0.4, 0.6, and 0.8%wt with 1.5%wt of Ru on anatase TiO_2 catalysts. XRD patterns were collected at the diffraction angles (2θ) between 20° to 80°. The XRD characteristic peaks of the crystalline phases of TiO_2 were detected. The TiO_2 anatase phase at 2θ = 25°(major), 37°, 48°, 55°, 56°, 62°, 71°, 75° and rutile phase at 27°(major), 36°, 42°, and 57° without formation of brookite phase, were observed for all the samples [42]. The peaks corresponding to Ru and Co were not detected probably because of low content of metal loading [52].

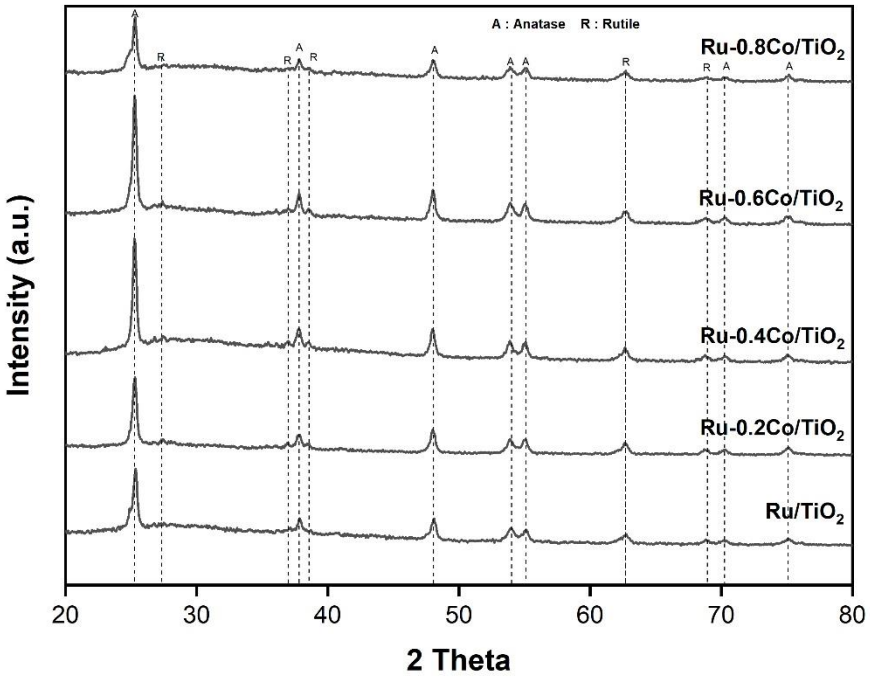

Figure 5.8 The XRD patterns of Ru-Co/TiO_2 catalysts with different Co contents

The 1.5%wt of Ru on TiO_2 catalysts prepared with different Co contents and 1.5%wt of Ru on TiO_2 catalyst displayed similar XRD patterns. The average crystallite size of anatase phase TiO_2 supports were calculated by the Scherrer's equation from the full width at half maximum of the XRD peak at 2θ = 25° (major). All the average crystallite size of anatase phase TiO_2 supports catalysts were similar about 28-32 nm as shown in Table 5.2

Table 5.6 shows the percentages of anatase and rutile phase of Ru/TiO_2 and $Ru\text{-}Co/TiO_2$ with different Co loading catalysts, there was no significant change in the percentage of anatase phase of TiO_2 of Ru/TiO_2, $Ru\text{-}0.2Co/TiO_2$, $Ru\text{-}0.4Co/TiO_2$, and $Ru\text{-}0.6Co/TiO_2$. On the other hand, the result showed the decreased of percentage of anatase phase at 93% for $Ru\text{-}0.8Co/TiO_2$ which may be due to high Co loading to Ru/TiO_2 causing large particle size of Ru.

Table 5.6 Ru/TiO_2 with different Co content samples consisting of various % Anatase

Sample	Anatase phase[a, b] (%)	Rutile phase[a, b] (%)
Ru/TiO_2	96	4
$Ru\text{-}0.2Co/TiO_2$	95	5
$Ru\text{-}0.4Co/TiO_2$	95	5
$Ru\text{-}0.6Co/TiO_2$	96	4
$Ru\text{-}0.8Co/TiO_2$	93	7

[a]Base on the XRD results.

[b]Determined from Jung et al. method.

5.3.2 N_2 Physisorption

The N_2 adsorption-desorption isotherms of Ru/TiO_2, $Ru\text{-}0.2Co/TiO_2$, $Ru\text{-}0.4Co/TiO_2$, $Ru\text{-}0.6Co/TiO_2$, and $Ru\text{-}0.8Co/TiO_2$ are shown in **Figure 5.9** According to the Brunauer-Deming-Deming-Teller (BDDT) classification of sorption isotherms, all catalysts showed type-IV N_2 adsorption-desorption isotherms with hysteresis loop at high relative pressure in the range of 0.8 to 1.0, which was the characteristic of mesoporous materials. The pore size of mesoporous material was in the range of 2-50

nm. The shape characteristic of hysteresis loop for all catalysts was type H3 indicating to the slit-like pores. So, the Co content between 0.2-0.8, that added to Ru/TiO_2 catalysts did not affect the structural properties of the catalyasts.

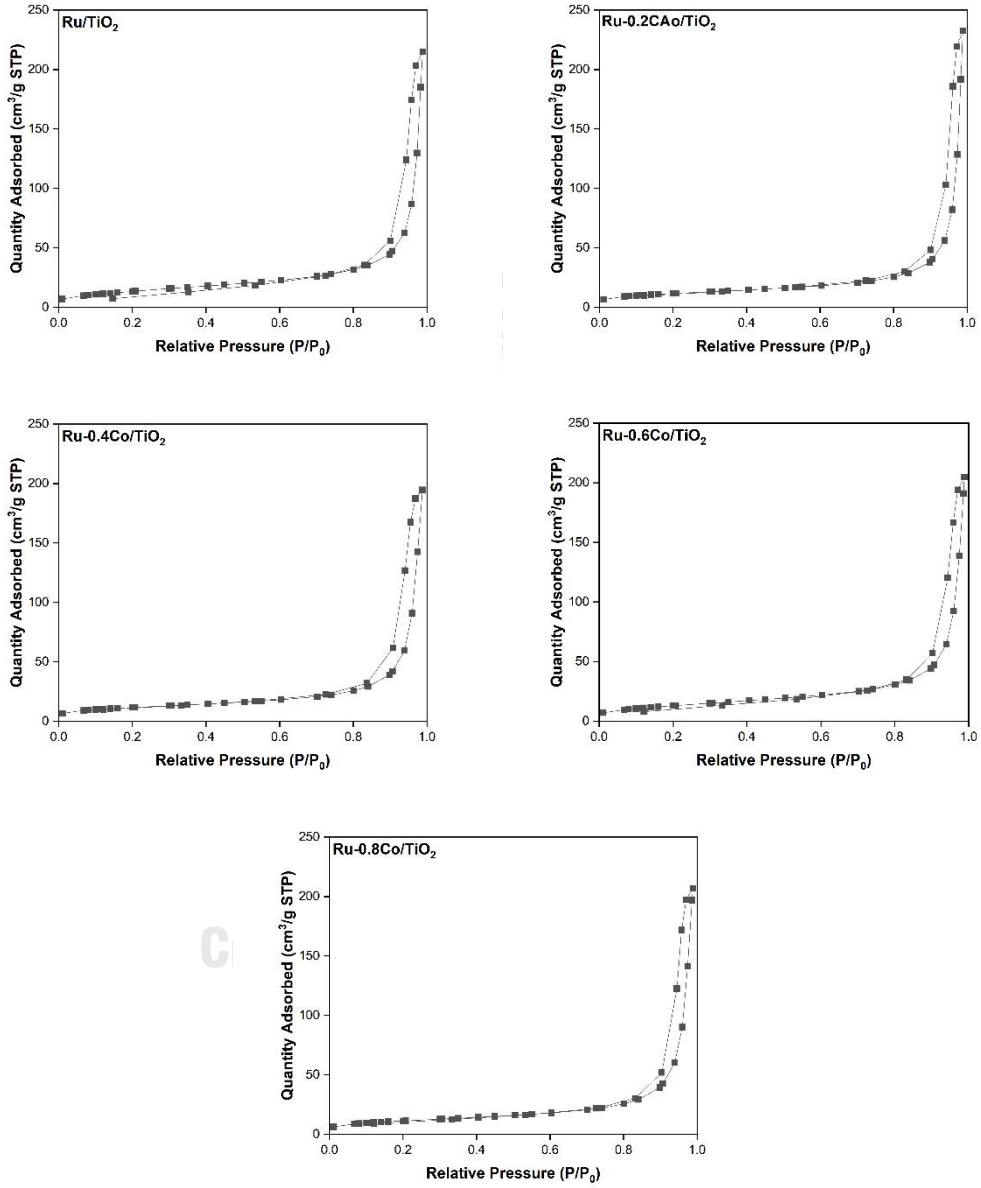

Figure 5.9 N_2-Physisorption isotherms of Ru/TiO_2, $Ru\text{-}0.2Co/TiO_2$, $Ru\text{-}0.4Co/TiO_2$, $Ru\text{-}0.6Co/TiO_2$, and $Ru\text{-}0.8Co/TiO_2$

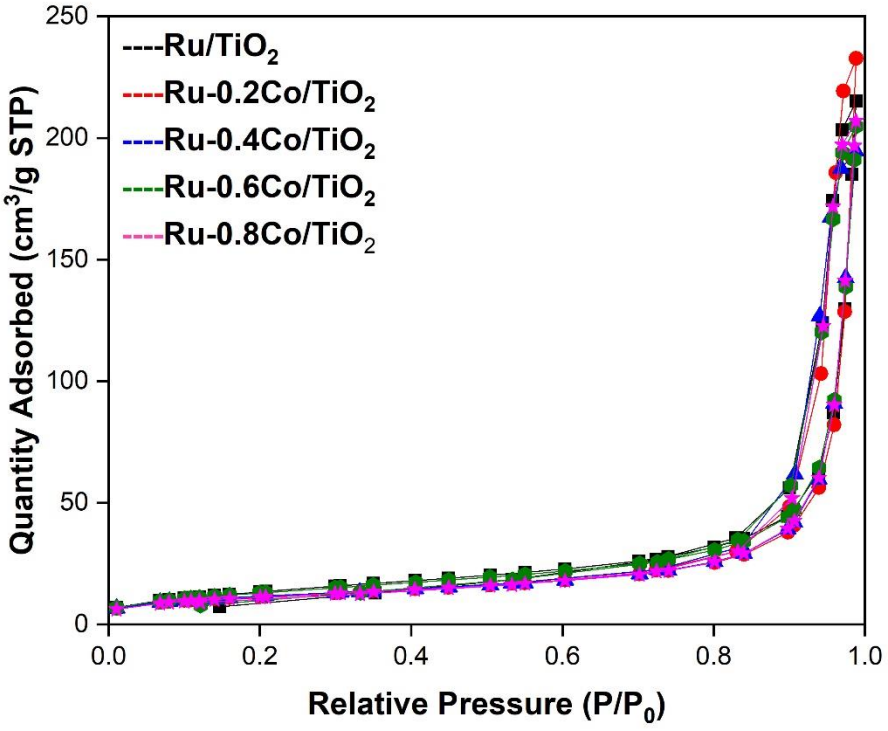

Figure 5.10 N_2-Physisorption isotherms of Ru/TiO_2, $Ru\text{-}0.2Co/TiO_2$, $Ru\text{-}0.4Co/TiO_2$, $Ru\text{-}0.6Co/TiO_2$, and $Ru\text{-}0.8Co/TiO_2$

The BET surface area, the average anatase TiO_2 crystallite size, pore volume, and pore size of the Ru/TiO_2 and $Ru\text{-}Co/TiO_2$ with different Co contents prepared by the incipient wetness impregnation method are shown in Table 5.7. The BET surface areas, pore volume, and pore size of Ru/TiO_2 and $Ru\text{-}Co/TiO_2$ with different Co contents were determined to be 41-50 m^2/g, 0.30-0.36 cm^3/g, 22-29 nm, respectively. The average anatase TiO_2 crystallite size of all catalysts were no significant different at around 28-32 nm.

Table 5.7 Physical properties of the Ru/TiO_2 and $Ru-Co/TiO_2$ with different Co content catalysts.

Sample	Avg. crystallite size[a] of anatase TiO_2 (nm)	BET surface area (m^2/g)	Pore volume[b] (cm^3/g)	Pore size[b] (nm)
Ru/TiO_2	27.9	50	0.32	22.0
$Ru-0.2Co/TiO_2$	27.9	42	0.36	29.2
$Ru-0.4Co/TiO_2$	30.7	42	0.30	23.8
$Ru-0.6Co/TiO_2$	30.7	45	0.31	22.3
$Ru-0.8Co/TiO_2$	32.4	41	0.32	25.9

[a]Base on the XRD results.

[b]Determined from the Barret-Joyner-Halenda (BJH) desorption method.

5.3.3 H_2-temperature programmed reduction

The H_2-TPR measurements were performed with all the catalysts in order to investigate the reducibility and the metal and support interaction of Ru/TiO_2 and $Ru-Co/TiO_2$ with different Co contents. The results are shown in **Figure5.11** The Ru/TiO_2, $Ru-0.2Co/TiO_2$, $Ru-0.4Co/TiO_2$, $Ru-0.6Co/TiO_2$, and $Ru-0.8Co/TiO_2$ catalysts presented three reduction peaks. The first sharp peak between 200°C and 250°C can be assigned to the reduction of Ru(III) to Ru(0) and the metal-metal interaction [53]. The second peak appeared broad peak between 400°C and 409°C can be assigned to the reduction of Ru interacting with TiO_2 [54]. The last peak was very broad peak around 720°C and 740°C which was interpreted as surface reduction of TiO_2 [38]. The H_2-TPR profile of Co/TiO_2 displayed two shoulder peaks at 371°C and 492°C and a main reduction peak at 440°C. The first shoulder peak was attributed to the reduction of Co precursor and the second main reduction peak was attributed to the two-step reduction of cobalt oxide: $Co_3O_4 \longrightarrow CoO \longrightarrow Co^0$. The last shoulder peak could be attributed to the interaction between Co and Ti and the peak at 742°C was interpreted as surface reduction of TiO_2 [38, 55].

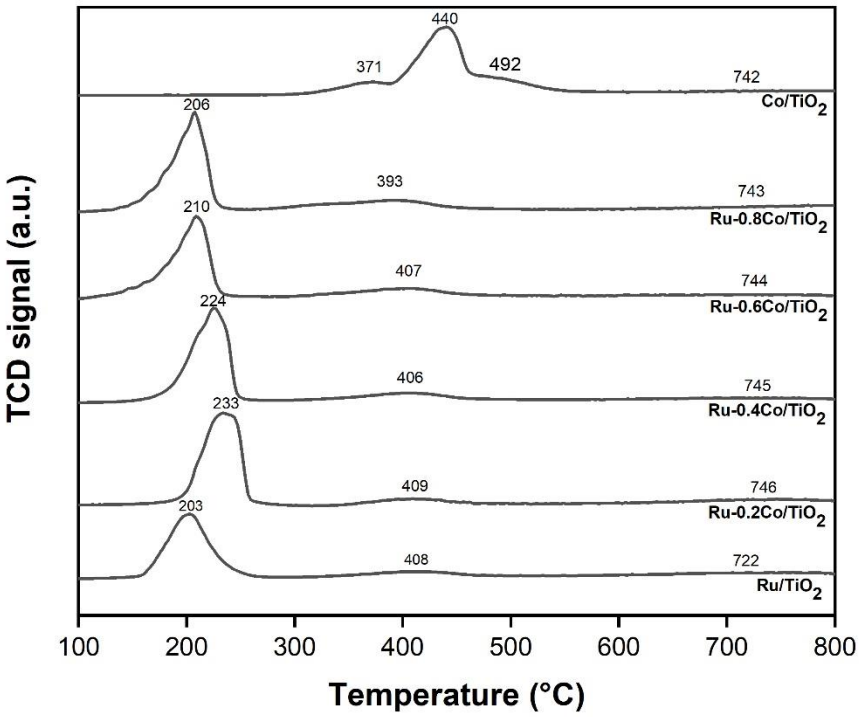

Figure 5.11 The H_2-TPR profiles of Ru/TiO_2, $Ru\text{-}Co/TiO_2$ with different Co content and Co/TiO_2 catalysts

Concerning the H_2-TPR profile of Ru/TiO_2, the reduction peak of Ru(III) to Ru(0) appeared at 203°C while the bimetallic $Ru\text{-}Co/TiO_2$ catalysts exhibited a shift of the reduction peaks of Ru(III) to Ru(0) towards higher temperature, suggesting stronger interaction between Ru and Co as also confirmed by XPS results in **Figure 5.15** for the Ru 3d peak in XPS spectra of Ru/TiO_2 with different Co contents. The reduction peaks of cobalt oxides were not detected in the TPR profiles of $Ru\text{-}Co/TiO_2$. The amount of Ru-Co interaction was maximized at 0.2 wt% Co content as the highest reduction temperature shift was observed at 233°C. Increasing Co content from 0.4, 0.6, and 0.8 wt%, the H_2-TPR profile showed the peak shift back to lower temperature [56, 57], which was due to the increasing size of the metal as also displayed in TEM image analysis [7, 9, 57]. There were no significant differences for the broad peaks at 406-408°C for all catalysts studied except the $Ru\text{-}0.8Co/TiO_2$ in which the peak was shifted to lower temperature at 393°C which suggested that

addition higher amount of Co at 0.8 wt% led to weaker interaction between Ru and TiO_2. Moreover, the adding of Co content resulted in higher peak area of the Ru reduction peaks due to the incorporation of Co species in the Ru.

5.3.4 Transmission electron microscopy (TEM)

The morphology and particle size of the particles can be estimated by using TEM method. The representative images of the Ru/TiO_2, and the bimetallic $Ru\text{-}Co/TiO_2$ catalysts with different Co contents are shown in **Figure 5.12** the TEM images of all the catalysts showed the nano-spherical particles with uniform particle size [39]. The average particle size of Ru on Ru/TiO_2, $Ru\text{-}0.2Co/TiO_2$, $Ru\text{-}0.4Co/TiO_2$, $Ru\text{-}0.6Co/TiO_2$, $Ru\text{-}0.6Co/TiO_2$ catalysts determined from the TEM images were approximately as 3.6, 4.5, 5.4, 5.8, 6.3 nm, respectively. The TEM results were in good agreement with the results of H_2-TPR and CO-pulse Chemisorption. The Ru particles of all catalysts were directly observed by TEM analysis for example the small dark spots be seen as Ru metal with the Co particles. However, at higher Co loading, $Ru\text{-}0.8Co/TiO_2$, the metallic clusters can be seen as dark patches.

The addition of Co in the Ru/TiO_2 catalysts were reported. The increasing of Co content caused the growing of average particles size of Ru particles. This increase in particle size can be assigned in part to the selective deposit of cobalt on ruthenium [9, 39], as confirmed by the TEM-EDX images in **Figure 5.13**, The EDX of the small dark spots confirmed the presence of both Ru and Co. The isolated Co particles were not observed in TEM image, it is suggested that all the Co particles were combined in the Ru particles, The TEM-EDX results were consistent to the X-ray photoelectron spectroscopy technique and the H_2-TPR results. Overall the TEM suggests that to form an active catalysts for this reaction larger Ru particles (4nm - 6 nm) are preferred.

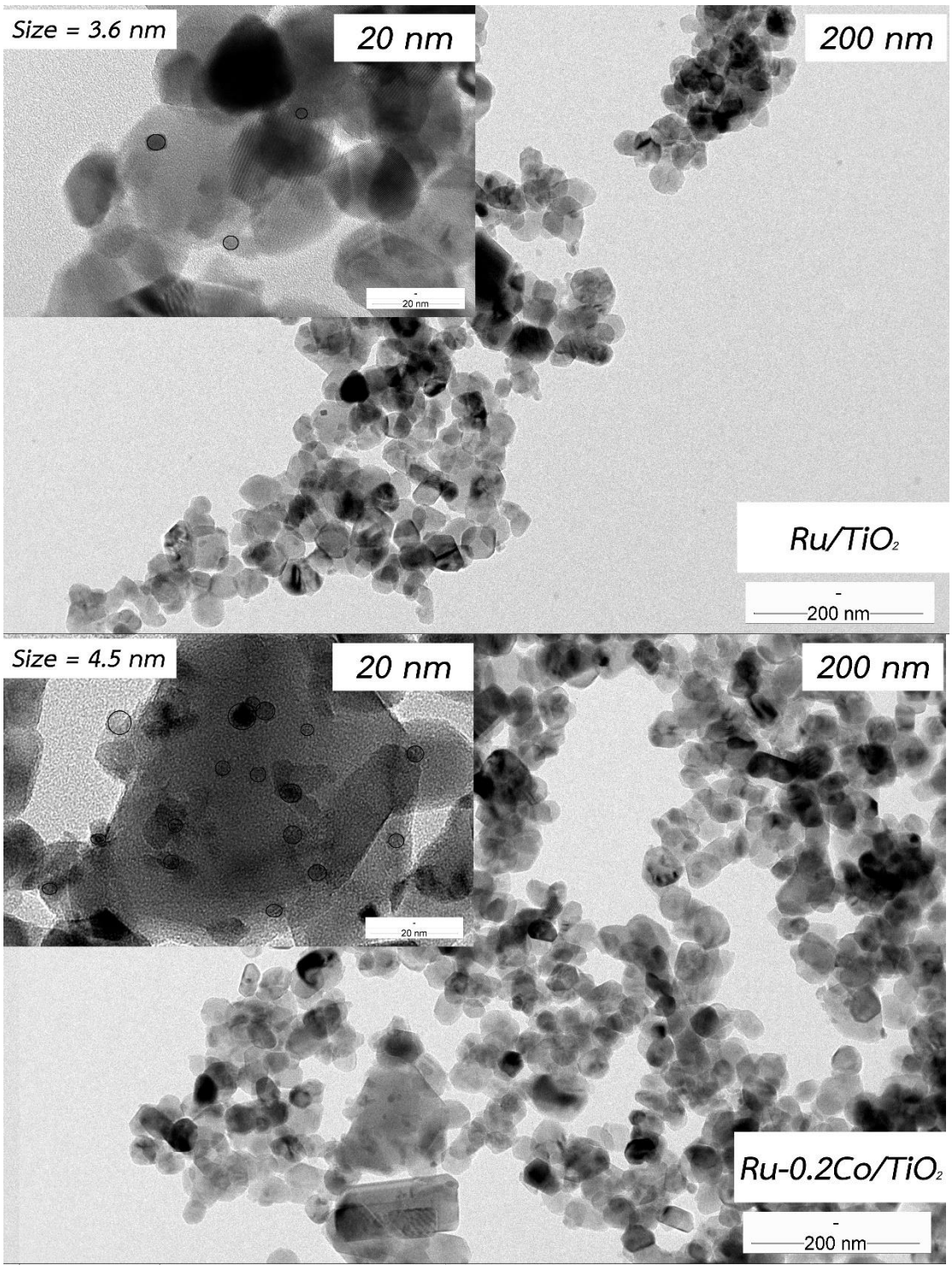
Size = 3.6 nm
20 nm
20 nm
200 nm
Ru/TiO2
200 nm
Size = 4.5 nm
20 nm
20 nm
200 nm
Ru-0.2Co/TiO2
200 nm

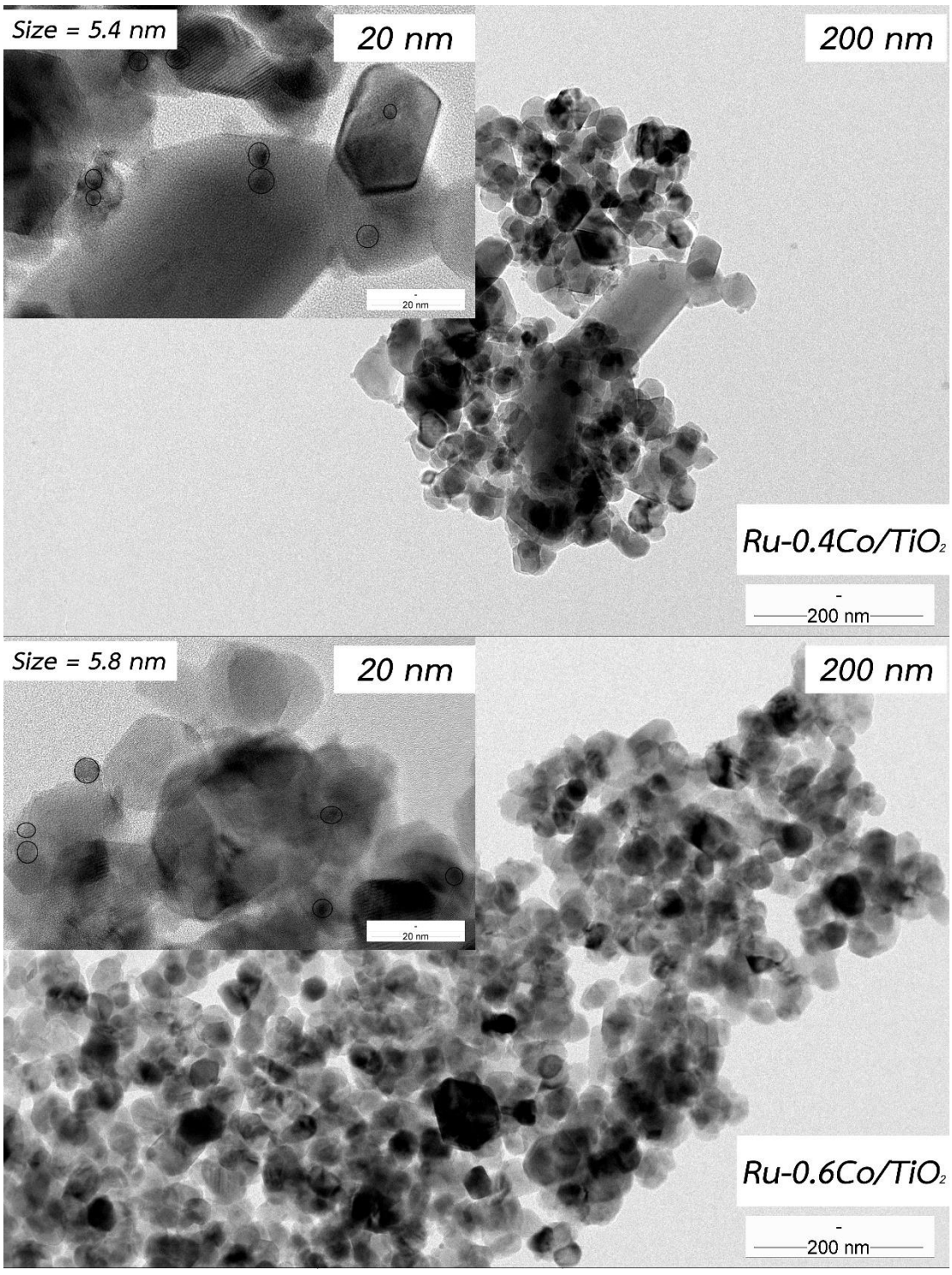
Size = 5.4 nm
20 nm
200 nm
Ru-0.4Co/TiO2
200 nm
Size = 5.8 nm
20 nm
200 nm
Ru-0.6Co/TiO2
200 nm

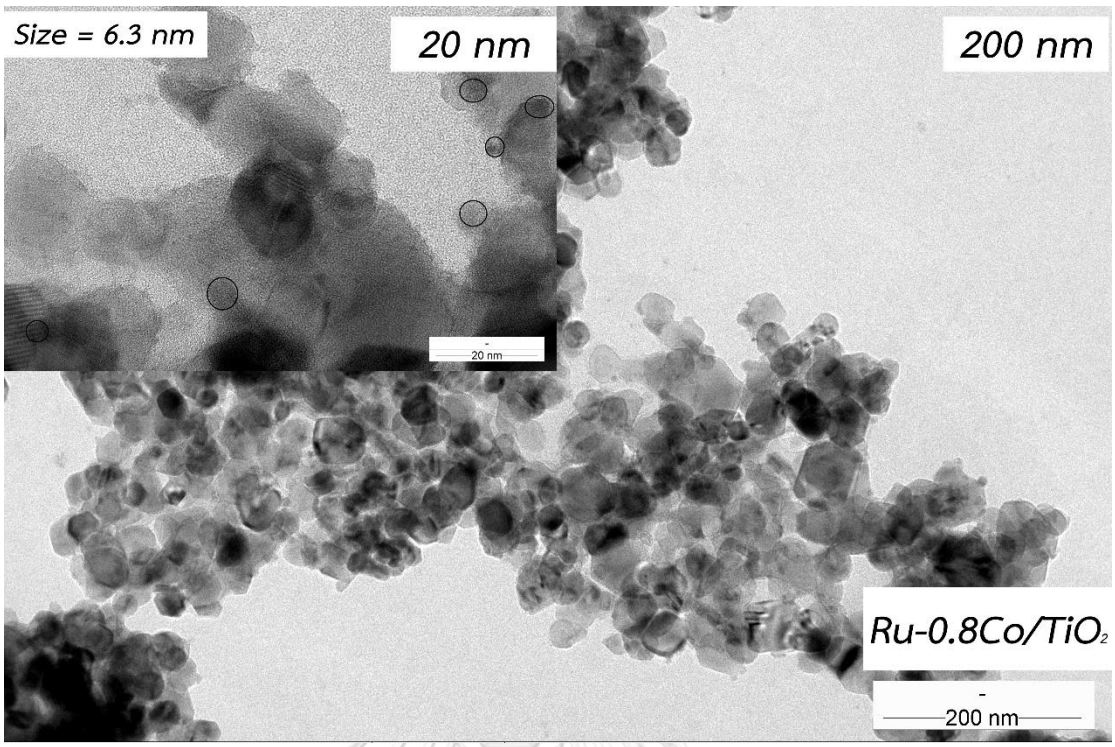

Figure 5.12 TEM images of Ru/TiO_2, $Ru\text{-}0.2Co/TiO_2$, $Ru\text{-}0.4Co/TiO_2$, $Ru\text{-}0.6Co/TiO_2$, and $Ru\text{-}0.8Co/TiO_2$

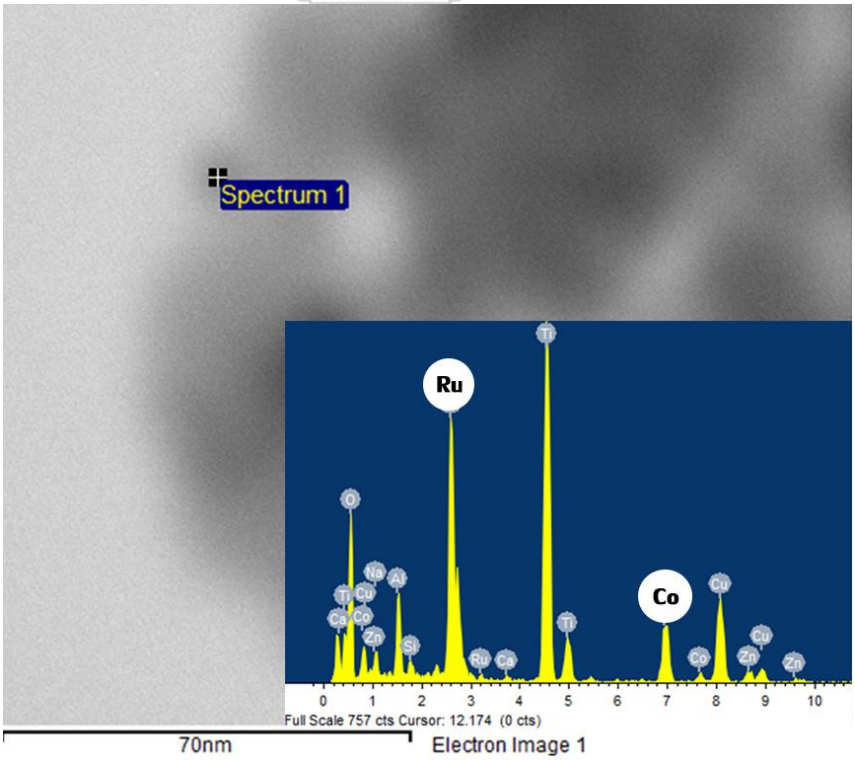

Figure 5.13 TEM-EDX images of $Ru\text{-}0.6Co/TiO_2$

5.3.5 X-ray photoelectron spectroscopy (XPS)

The XPS elemental survey scans of the surface technique were performed to determine the elemental composition of the catalyst sample at surface. The XPS results are shown in **Figure 5.14**. The C1s spectrum was observed at binding energies of 284.8 eV. There was a strong overlap of the C1s and Ru3d peaks at around 248.8eV was therefore it complicated to deconvolute the peaks because carbon peak overlap with the Ru $3d_{3/2}$ photoemission. From **Figure 5.15,** the deconvolution of Ru3d XPS peaks showed the main ruthenium species $Ru3d_{5/2}$ located at 280.8eV [58]. The XPS signal for the sample was weak because of the low loading of metal. The increasing of Co content in Ru/TiO_2 catalyst was reported to the shifting of binding energies of $Ru3d_{5/2}$ peak. The shift towards higher binding energy with the energy difference of 2eV approximately of $Ru3d_{5/2}$ peak (Ru/TiO_2 to $Ru\text{-}0.8Co/TiO_2$) can be observed for $Ru\text{-}Co/TiO_2$ catalyst relative to the monometallic Ru-based catalyst at 280.8 eV, indicating the formation of Ru and Co interaction [59, 60] and/or may be formation of Ru-Co alloy in the $Ru\text{-}Co/TiO_2$ catalyst [61]. This conclusions are in good agreement with the H_2-TPR analysis and TEM images.

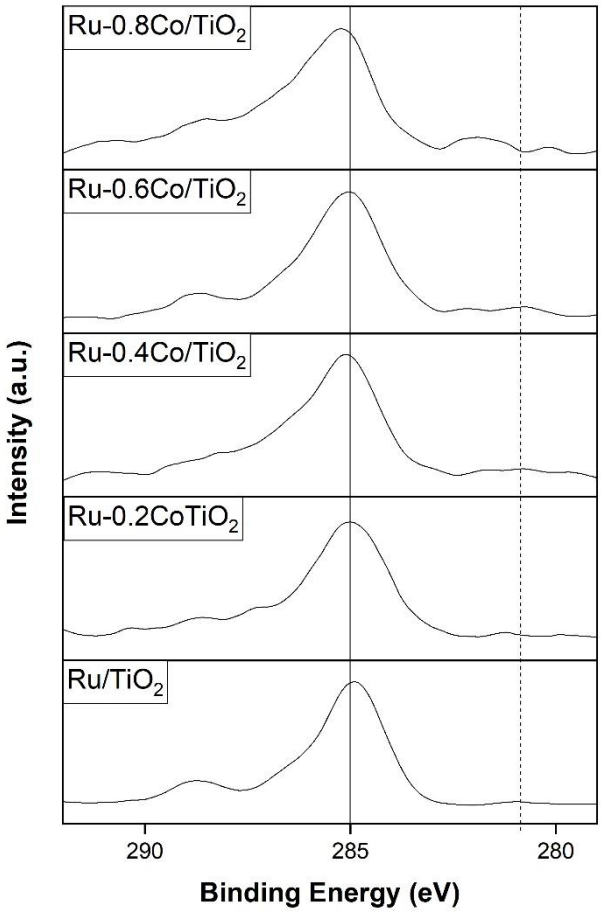

Figure 5.14 Overall Ru peak in XPS spectra of Ru/TiO_2 with different Co content

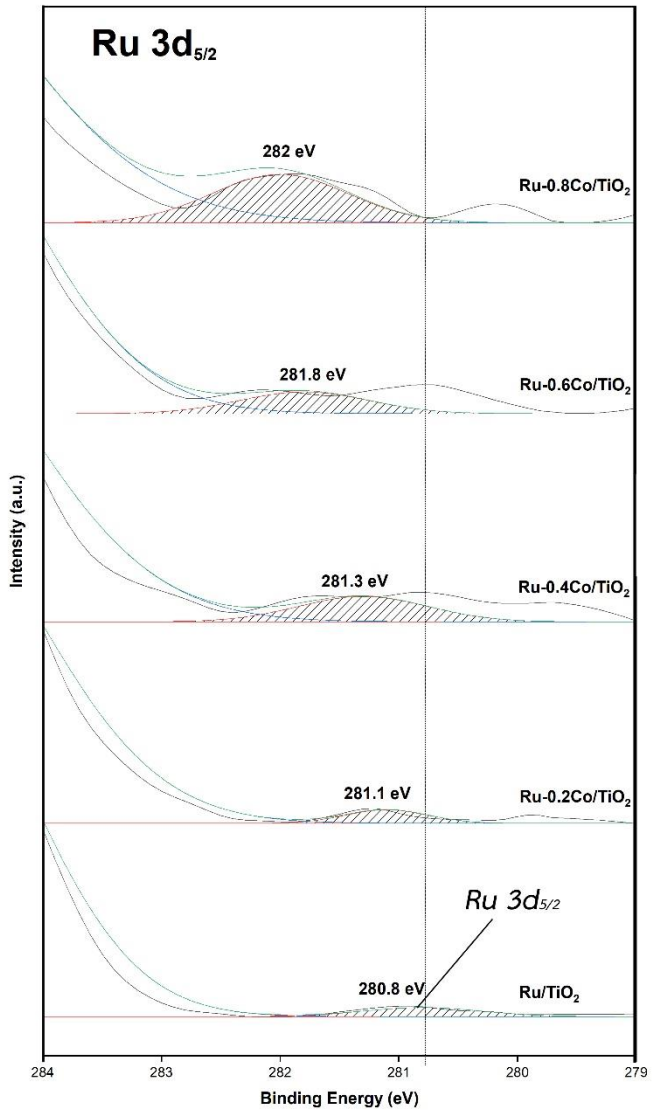

Figure 5.15 Ru 3d peak in XPS spectra of Ru/TiO_2 with different Co content

5.3.6 CO-pulse Chemisorption

The amounts of CO adsorbed on the Ru/TiO_2 with different Co contents and percentage of Ru dispersion on TiO_2 support were estimated by the chemisorption based on the assumption CO : Ru = 1 : 1. It can be observed from **Table5.8**, the Ru/TiO_2, $Ru\text{-}0.2Co/TiO_2$, $Ru\text{-}0.4Co/TiO_2$, $Ru\text{-}0.6Co/TiO_2$, and $Ru\text{-}0.8Co/TiO_2$ catalysts showed the Ru dispersion at 1.5%, 0.9%, 0.8%, 0.8%, and 0.7%, consecutively. The increasing amount of Co loading on Ru/TiO_2 catalysts resulted in slightly lower Ru dispersion because of the particle size of Ru affected to Ru dispersion [39, 45]. The

CO-pulse chemisorption results also corresponded well to the TEM images and the H_2-TPR results. So, the particle size of Ru was considered as the important of factor that affected the catalytic performances.

Table 5.8 CO chemisorption and metal concentrations of Ru/TiO_2 with different Co loading.

Catalysts	CO chemisorption (molecule CO × 10^{17}/g cat.)	Ru dispersion[a, b] (%)
Ru/TiO_2	13.4	1.5
$Ru\text{-}0.2Co/TiO_2$	8.1	0.9
$Ru\text{-}0.4Co/TiO_2$	7.2	0.8
$Ru\text{-}0.6Co/TiO_2$	7.1	0.8
$Ru\text{-}0.8Co/TiO_2$	6.3	0.7

[a] Determined from 1.5% of Ru

[b] Determined from CO-pulse chemisorption technique with the chemisorption based on the assumption CO : Ru = 1 : 1

5.3.7 Scanning electron microscopy and energy dispersive X-ray spectroscopy (SEM-EDX)

SEM images for the Ru/TiO_2, $Ru\text{-}0.2Co/TiO_2$, $Ru\text{-}0.4Co/TiO_2$, $Ru\text{-}0.6Co/TiO_2$, and $Ru\text{-}0.8Co/TiO_2$ nanocrystalline structures are shown in **Figure 5.16**. The results showed no significant change of morphology and characteristic shape and were allowed identifying the individual nanoscale globular or nearly spherical particles for all catalysts [62]. Elemental analysis by EDX indicated that the chemical compositions were close to stoichiometrical percentages of Ru around 1.5% of all catalysts and slightly increased percentages of Co around 0.6 and 1.5 of $Ru\text{-}0.2Co/TiO_2$ and $Ru\text{-}0.8Co/TiO_2$.

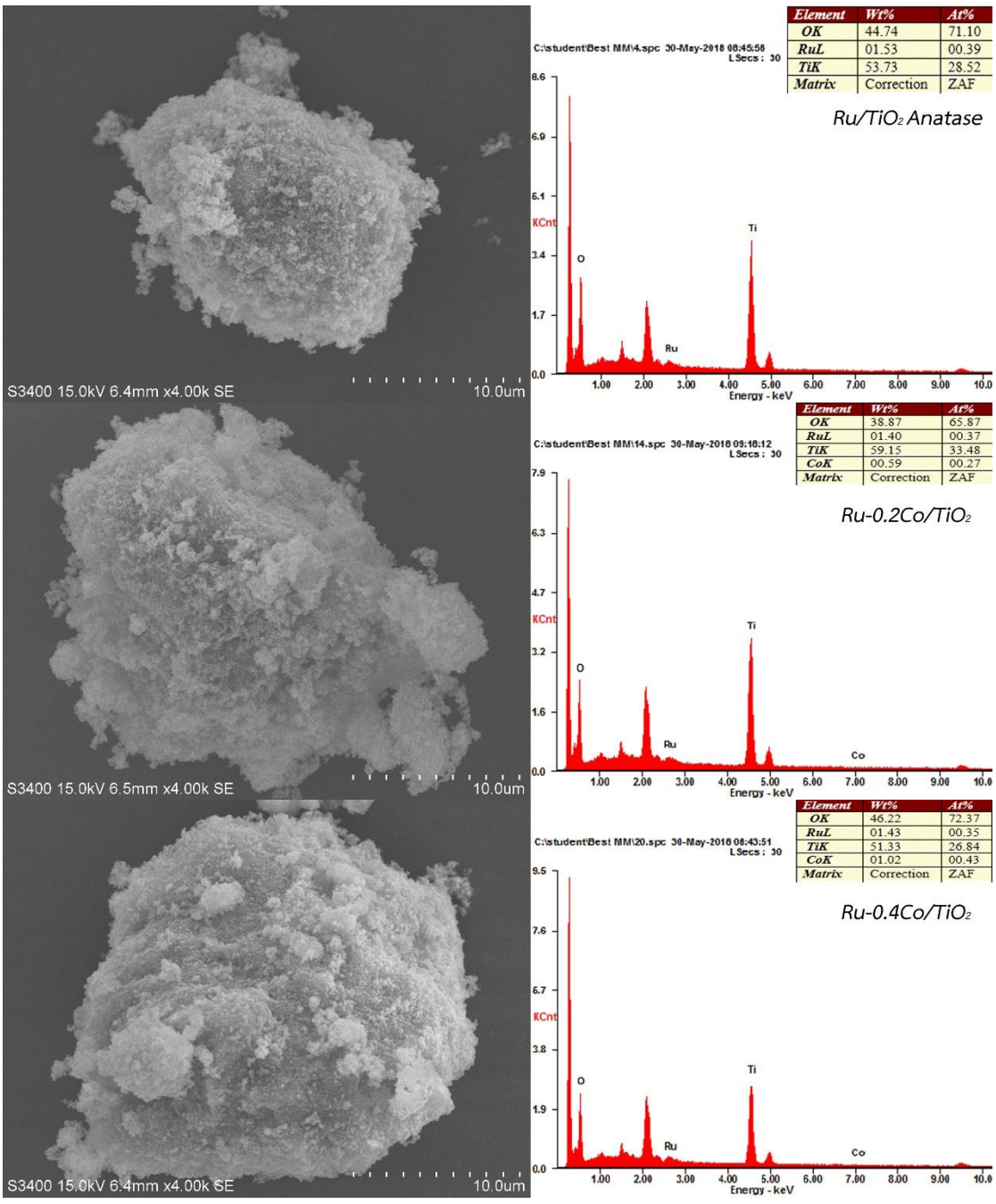
S3400 15.0kV 6.4mm x4.00k SE
10.0um
C:\student\Best MM\4.spc 30-May-2018 08:45:58
LSecs : 30
Element | Wt% | At%
OK | 44.74 | 71.10
RuL | 01.53 | 00.39
TiK | 53.73 | 28.52
Matrix | Correction | ZAF
Ru/TiO2 Anatase
KCnt
O
Ti
Ru
Energy - keV
S3400 15.0kV 6.5mm x4.00k SE
10.0um
C:\student\Best MM\14.spc 30-May-2018 09:16:12
LSecs : 30
Element | Wt% | At%
OK | 38.87 | 65.87
RuL | 01.40 | 00.37
TiK | 59.15 | 33.48
CoK | 00.59 | 00.27
Matrix | Correction | ZAF
Ru-0.2Co/TiO2
KCnt
O
Ti
Ru
Co
Energy - keV
S3400 15.0kV 6.4mm x4.00k SE
10.0um
C:\student\Best MM\20.spc 30-May-2018 08:43:51
LSecs : 30
Element | Wt% | At%
OK | 46.22 | 72.37
RuL | 01.43 | 00.35
TiK | 51.33 | 26.84
CoK | 01.02 | 00.43
Matrix | Correction | ZAF
Ru-0.4Co/TiO2
KCnt
O
Ti
Ru
Co
Energy - keV

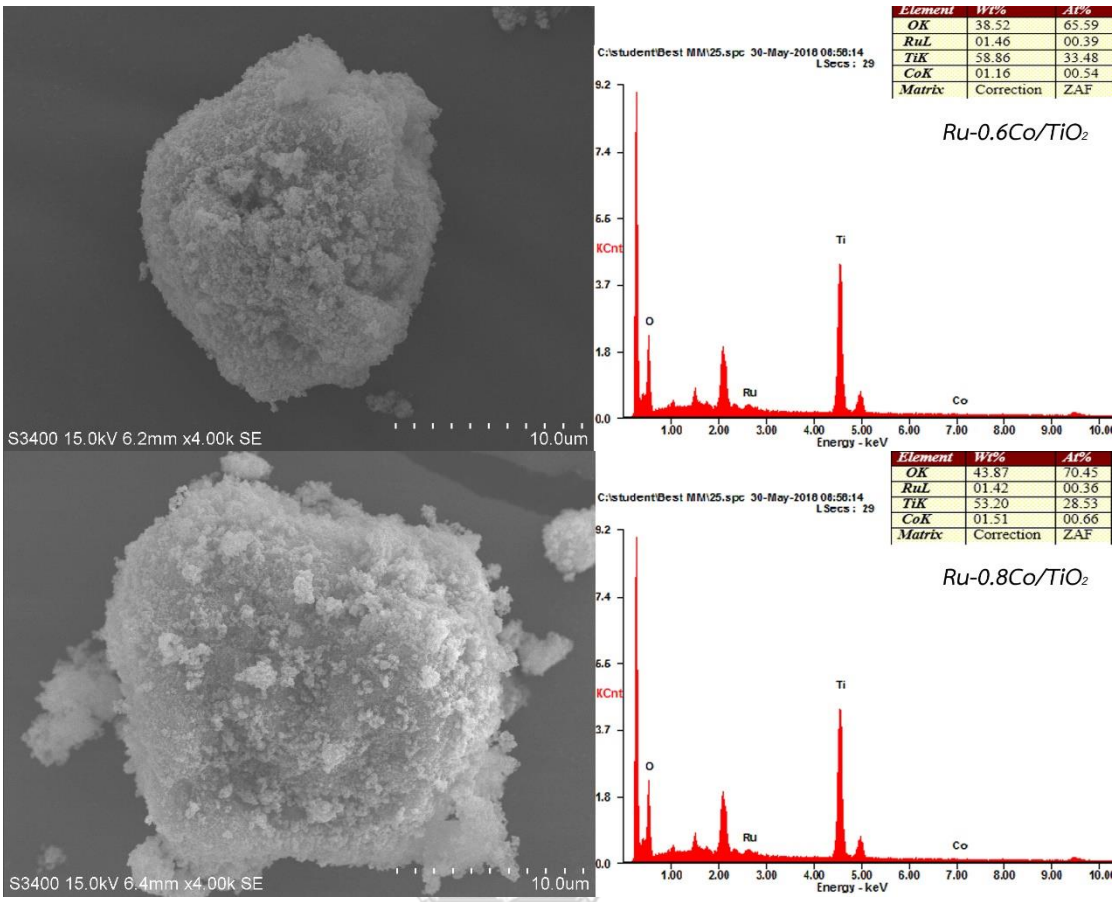

Figure 5.16 The SEM-EDX of Ru/TiO_2 and $Ru\text{-}Co/TiO_2$ with different Co content catalysts

5.4 The catalytic performances of Ru/TiO_2 with different Co content in the liquid-phase furfural hydrogenation

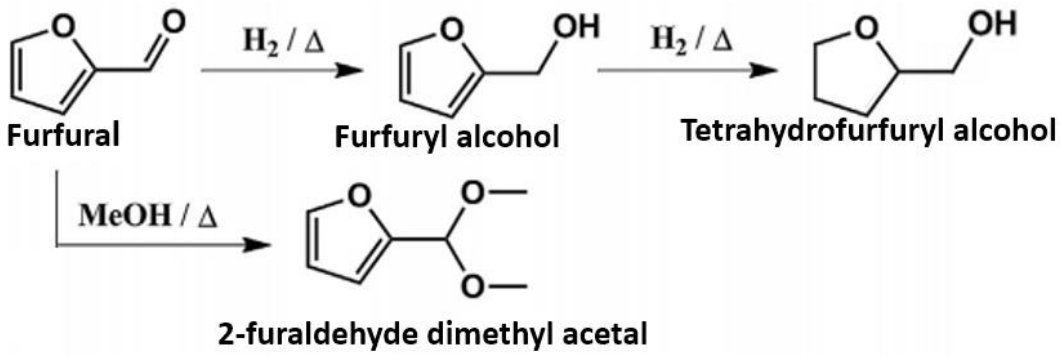

Figure 5.17 The pathway of furfural hydrogenation reaction

The catalytic performances of 1.5%Ru/TiO $_2$and 1.5%Ru-Co/TiO $_2$with different Co contents at 0.2, 0.4, 0.6, and 0.8 catalysts were investigated in the selective hydrogenation of furfural under the following reaction conditions temperature at 50°C, H_2 pressure 20 bar, and 2h reaction time. The catalytic behaviors of 1.5%Ru/TiO $_2$and 1.5%Ru-Co/TiO $_2$with different Co contents at 0.2, 0.4, 0.6, and 0.8 catalysts following furfural conversion and selectivity of furfuryl alcohol are summarized in **Table5.17**. The main product was furfuryl alcohol and the by-product was 2-furaldehyde dimethyl acetal. The main product furfuryl alcohol was not hydrogenated to tetrahydrofurfuryl alcohol probably due to the short reaction time and/or the characteristic of Ru/TiO_2 catalysts [48]. From the results, the addition amount of Co loading in the Ru/TiO_2 displayed the increasing of catalytic activity in terms conversion with slightly change in the selectivity of furfuryl alcohol for all the amounts of Co loading in the Ru/TiO_2 due to the Ru-Co interaction. The increasing of catalytic activity when the amount of Co loading were added to Ru/TiO_2 could be attributed to the increasing of Ru-Co alloy interaction [63] and the optimum of size of Ru particles as observed at TEM images. From the TEM images, it was noticed that the increasing of Co content caused the growing of average particles size of Ru particles, which were suggested to be more active for this reaction. The TEM results were in good agreement with the results of H_2-TPR, CO-pulse chemisorption and XPS. The individual Co particles were not observed in TEM images. Thus, the Co particles was combined in the Ru particles, which was also supported by the X-ray photoelectron spectroscopy technique in **Figure5.15**, The shift towards higher binding energy of $Ru3d_{5/2}$ peak can be estimated for $Ru-Co/TiO_2$ catalyst relative to the monometallic Ru-based catalyst at 280.8 eV, indicating the formation of Ru and Co interaction [59, 60] and/or may be formation of Ru-Co alloy in the $Ru-Co/TiO_2$ catalyst [61]. The interaction of Ru–Co bimetallic showed better performance than pure Ru in catalyzing hydrogen evolution [64]. CO-pulse chemisorption showed the decreasing of Ru dispersion because the particle size of Ru affected to Ru dispersion. The H_2-TPR of catalyst after loading the amount of Co to Ru/TiO_2 was performed the shift back to lower temperature [56, 57] which was due to the increasing size of the Ru metal and Ru-Co alloy formation [63]. The H_2-TPR peak did not show the peak of Co reduction. In addition, the interaction of Ru and Co

resulted in higher peak area of the Ru reduction peaks due to the incorporation of Co species in the Ru reduction peaks. From, the results of H_2-TPR, TEM images, CO-pulse chemisorption, and XPS, it can be summarized that the increasing of Ru particle size by interaction between Ru and Co on the TiO_2 support improved the catalytic activity of Ru/TiO_2 catalysts in terms of conversion.

On the other hand, the conversion of $Ru\text{-}0.8Co/TiO_2$ was decreased because the Ru particles size may be too large as supported by the H_2-TPR and/or the percentages of anatase of TiO_2 that was the lowest among all the catalysts. The percentages of anatase of TiO_2 could affect the catalytic activity because the anatase phase of TiO_2 are favorable adsorption sites for hydrogen atoms [49, 50]. Moreover, the anatase phase of TiO_2 slightly affected to the increase in the selectivity of furfuryl alcohol from 90% of the pure Ru/TiO_2 to 96% of Co loading in the Ru/TiO_2 catalysts.

Table 5.9 Conversion of furfural and selectivity to furfuryl alcohol of Ru/TiO_2 with different Co contents

Catalysts	Conversion (%)	Selectivity to FA[a]	Selectivity to SP[b]
Ru/TiO_2	31.8	90.0	10.0
$Ru\text{-}0.2Co/TiO_2$	56.9	95.7	4.3
$Ru\text{-}0.4Co/TiO_2$	81.2	95.7	4.3
$Ru\text{-}0.6Co/TiO_2$	91.7	97.5	2.5
$Ru\text{-}0.8Co/TiO_2$	86.4	96.1	3.9

Reaction (50μL furfural in 10 ml methanol) at 50°C under 20 bay H_2 with a 50 mg catalyst in 120 min

[a] Selectivity of furfuryl alcohol

[b] Selectivity of 2-furaldehyde dimethyl acetal

CHAPTER VI
CONCLUSIONS

6.1 Conclusions

1) The Ru/TiO_2 prepared with various phases of TiO_2 exhibited different average TiO_2 crystallite size, BET surface area, pore volume, and average pore size. The H_2-TPR results of the Ru/TiO_2 prepared with different phases of TiO_2 showed a shift of Ru and TiO_2 peaks, suggesting in the weak Ru and TiO_2 support interaction. It was found that the anatase phase TiO_2 could enhance the catalytic activity and H_2 consumption of Ru-TiOx interface species could increase the selectivity of furfuryl alcohol. The Ru/TiO_2-A with 97% anatase phase of TiO_2 showed the best catalytic activity at conversion of furfural (30%) and selectivity of furfuryl alcohol (90%) under the reaction conditions used. The anatase phase TiO_2 is suggested to be favorable adsorption sites for hydrogen atoms so that hydrogenation activity increases.

2) The addition of Co to the Ru/TiO_2 catalysts, resulted in the improved catalytic performances in terms of conversion and selectivity with the Ru-0.6Co/TiO_2 catalyst displayed the highest conversion of furfural (90%) with high selectivity to furfuryl alcohol (>90%). The improved catalytic activity by loading of Co content was correlated to H_2-TPR, TEM, and XPS results. The increasing of Ru particles size, the Ru-Co alloy interaction, and the strong interaction between Ru and Co led to superior catalytic performances of the bimetallic Ru-Co catalysts compared to the monometallic one.

6.2 Recommendation

1. The interaction between Ru and Co should be further investigated by high sophisticated techniques such as EXAFS.

2. The solvent in hydrogenation of furfural that does not produce solvent product should be researched.

REFERENCES

[1] L. Liu, H. Lou, and M. Chen, "Selective hydrogenation of furfural over Pt based and Pd based bimetallic catalysts supported on modified multiwalled carbon nanotubes (MWNT)," *Applied Catalysis A: General,* vol. 550, pp. 1-10, 2018.

[2] L. Liu *et al.*, "Mechanism and kinetics of the electrocatalytic hydrogenation of furfural to furfuryl alcohol," *Journal of Electroanalytical Chemistry,* vol. 804, pp. 248-253, 2017.

[3] G. Pahla, T. A. Mamvura, F. Ntuli, and E. Muzenda, "Energy densification of animal waste lignocellulose biomass and raw biomass," *South African Journal of Chemical Engineering,* vol. 24, pp. 168-175, 2017.

[4] C. Zhang, Q. Lai, and J. H. Holles, "Bimetallic overlayer catalysts with high selectivity and reactivity for furfural hydrogenation," *Catalysis Communications,* vol. 89, pp. 77-80, 2017.

[5] Q. Yuan *et al.*, "Selective liquid phase hydrogenation of furfural to furfuryl alcohol by Ru/Zr-MOFs," *Journal of Molecular Catalysis A: Chemical,* vol. 406, pp. 58-64, 2015.

[6] R. M. Mironenko *et al.*, "Effect of the nature of carbon support on the formation of active sites in Pd/C and Ru/C catalysts for hydrogenation of furfural," *Catalysis Today,* vol. 249, pp. 145-152, 2015.

[7] O. F. Aldosari *et al.*, "Pd–Ru/TiO_2 catalyst – an active and selective catalyst for furfural hydrogenation," *Catalysis Science & Technology,* vol. 6, no. 1, pp. 234-242, 2016.

[8] C. Rizhi, D. Yan, X. Weihong, and X. Nanping, "The Effect of Titania Structure on Ni/TiO_2 Catalysts for p-Nitrophenol Hydrogenation," *Chemical Engineering,* vol. 14, no. 5, pp. 665-669, 2006.

[9] J. J. Musci, A. B. Merlo, and M. L. Casella, "Aqueous phase hydrogenation of furfural using carbon-supported Ru and RuSn catalysts," *Catalysis Today,* vol. 296, pp. 43-50, 2017.

[10] M. M. Byranvand, A. N. Kharat, L. Fatholahi, and Z. M. Beiranvand, "A review on synthesis of nano-TiO_2 via Different Methods," *Nanostructures,* vol. 3, pp. 1-9, 2013.

[11] T. Mashimo *et al.*, "Structure of Single-Crystal Rutile (TiO_2) Prepared by High-Temperature Ultracentrifugation," *Crystal Growth & Design,* vol. 17, no. 4, pp. 1460-1464, 2017.

[12] D. T. Croner and K. Herrington, "The Structures of Anatase and Rutile," *Am Chem Soc,* vol. 77, pp. 4708-4709, 1955.

[13] E. Morra, E. Giamello, and M. Chiesa, "EPR approaches to heterogeneous catalysis. The chemistry of titanium in heterogeneous catalysts and photocatalysts," *J Magn Reson,* vol. 280, pp. 89-102, Jul 2017.

[14] S. Bagheri, N. Muhd Julkapli, and S. Bee Abd Hamid, "Titanium dioxide as a catalyst support in heterogeneous catalysis," *ScientificWorldJournal,* vol. 2014, p. 727496, 2014.

[15] S.-Y. Wang, S. H. Moon, and M. A. Vannice, "The Effect of SMSI (Strong Meta ,I - Support Interaction) Behavior on CO Adsorption and Hydrogenation on Pd Catalysts " *Journal of catalysis,* vol. 71, pp. 167-174, 1981.

[16] M. M. Pereira, F. B. Noronha, and M. Schmal, "SMSI effect in the butadiene hydrogenation bimetallic catalysts " *Catalysis Today,* vol. 16, pp. 407-415, 1993.

[17] X. Cui *et al.*, "Highly selective hydrogenation of arenes using nanostructured ruthenium catalysts modified with a carbon–nitrogen matrix," *Nature Communications,* vol. 7, 2016.

[18] M. Mansouri, H. Atashi, and A. A. Mirzaei, "Hydrogenation of CO on Cobalt Catalyst in Fischer–Tropsch Synthesis," *Journal of Thermodynamics & Catalysis,* vol. 03, no. 02, 2012.

[19] R. R. C. M. Silva *et al.*, "Effect of support on methane decomposition for hydrogen production over cobalt catalysts," *International Journal of Hydrogen Energy,* vol. 41, no. 16, pp. 6763-6772, 2016.

[20] N. Mizuno and M. Makoto, "Heterogeneous Catalysis," *Chemical Reviews,* vol. 98, pp. 199-217, 1998.

[21] X. Chen, L. Zhang, B. Zhang, X. Guo, and X. Mu, "Highly selective hydrogenation of furfural to furfuryl alcohol over Pt nanoparticles supported on g-C_3N_4 nanosheets catalysts in water," *Sci Rep,* vol. 6, p. 28558, Jun 22 2016.

[22] R. V. Sharma, U. Das, R. Sammynaiken, and A. K. Dalai, "Liquid phase chemo-selective catalytic hydrogenation of furfural to furfuryl alcohol," *Applied Catalysis A: General,* vol. 454, pp. 127-136, 2013.

[23] H. Chen, H. Ruan, X. Lu, J. Fu, T. Langrish, and X. Lu, "Efficient catalytic transfer hydrogenation of furfural to furfuryl alcohol in near-critical isopropanol over Cu/MgO-Al_2O_3 catalyst," *Molecular Catalysis,* vol. 445, pp. 94-101, 2018.

[24] D. Vargas-Hernández *et al.*, "Furfuryl alcohol from furfural hydrogenation over copper supported on SBA-15 silica catalysts," *Journal of Molecular Catalysis A: Chemical,* vol. 383-384, pp. 106-113, 2014.

[25] M. M. Villaverde, N. M. Bertero, T. F. Garetto, and A. J. Marchi, "Selective liquid-phase hydrogenation of furfural to furfuryl alcohol over Cu-based catalysts," *Catalysis Today,* vol. 213, pp. 87-92, 2013.

[26] S. Bhogeswararao and D. Srinivas, "Catalytic conversion of furfural to industrial chemicals over supported Pt and Pd catalysts," *Journal of Catalysis,* vol. 327, pp. 65-77, 2015.

[27] Á. O'Driscoll, J. J. Leahy, and T. Curtin, "The influence of metal selection on catalyst activity for the liquid phase hydrogenation of furfural to furfuryl alcohol," *Catalysis Today,* vol. 279, pp. 194-201, 2017.

[28] Y. Li *et al.*, "The effect of titania polymorph on the strong metal-support interaction of Pd/TiO_2 catalysts and their application in the liquid phase selective hydrogenation of long chain alkadienes," *Journal of Molecular Catalysis A: Chemical,* vol. 216, no. 1, pp. 107-114, 2004.

[29] J. Panpranot, K. Kontapakdee, and P. Praserthdam, "Effect of TiO_2 Crystalline Phase Composition on the Physicochemical and Catalytic Properties of

Pd/TiO_2 in Selective Acetylene Hydrogenation," *The Journal of Physical Chemistry B,* vol. 110, pp. 8019-8024, 2006.

[30] P. Panagiotopoulou, N. Martin, and D. G. Vlachos, "Effect of hydrogen donor on liquid phase catalytic transfer hydrogenation of furfural over a Ru/RuO_2/C catalyst," *Journal of Molecular Catalysis A: Chemical,* vol. 392, pp. 223-228, 2014.

[31] P. Panagiotopoulou and D. G. Vlachos, "Liquid phase catalytic transfer hydrogenation of furfural over a Ru/C catalyst," *Applied Catalysis A: General,* vol. 480, pp. 17-24, 2014.

[32] J. Yang, J. Ma, Q. Yuan, P. Zhang, and Y. Guan, "Selective hydrogenation of furfural on Ru/Al-MIL-53: a comparative study on the effect of aromatic and aliphatic organic linkers," *RSC Advances,* vol. 6, no. 95, pp. 92299-92304, 2016.

[33] K. Fulajtárova, T. Soták, M. Hronec, I. Vávra, E. Dobročka, and M. Omastová, "Aqueous phase hydrogenation of furfural to furfuryl alcohol over Pd–Cu catalysts," *Applied Catalysis A: General,* vol. 502, pp. 78-85, 2015.

[34] L. Mao, Q. Li, H. Dang, and Z. Zhang, "Synthesis of nanocrystalline TiO_2 with high photoactivity and large specific surface area by sol–gel method," *Materials Research Bulletin,* vol. 40, no. 2, pp. 201-208, 2005.

[35] D.-S. Bae, K.-S. Han, and S.-H. Choi, "Fabrication and characterization of Ru-doped TiO_2, composite membranes by the sol-gel process " *Materials Letters* vol. 33, pp. 101-105, 1997.

[36] D. K. Mishra, J.-M. Lee, J.-S. Chang, and J.-S. Hwang, "Liquid phase hydrogenation of d-glucose to d-sorbitol over the catalyst (Ru/NiO–TiO_2) of ruthenium on a NiO-modified TiO_2 support," *Catalysis Today,* vol. 185, no. 1, pp. 104-108, 2012.

[37] J. Fontana, C. Vignado, E. Jordao, F. C. A. Figueiredo, and W. A. Carvalho, "Evaluation of some supports to RuSn catalysts applied to dimethyl adipate hydrogenation," *Catalysis Today,* vol. 172, no. 1, pp. 27-33, 2011.

[38] A. A. WISMEIJER, A. P. G. KIEBOOM, and H. V. BEKKUM, "SELECTIVE HYDROGENATION OF CITRONELLAL TO CITRONELLOL OVER Ru/TiOp AS COMPARED TO Ru/SiO_2 " *Applied Catalysis,* vol. 25, pp. 181-189, 1986.

[39] V. P. Kumar, Y. Harikrishna, N. Nagaraju, and K. V. R. Chary, "Characterization and reactivity of TiO_2 supported nano ruthenium catalysts for vapour phase hydrogenolysis of glycerol," *Indian Journal of Chemistry,* vol. 53A, pp. 516-523, 2014.

[40] T. Niu, G. L. Liu, and Y. Liu, "Preparation of Ru/graphene-meso-macroporous SiO_2 composite and their application to the preferential oxidation of CO in H_2-rich gases," *Applied Catalysis B: Environmental,* vol. 154-155, pp. 82-92, 2014.

[41] P. R. Upadhyay and V. Srivastava, "Selective hydrogenation of CO_2 gas to formic acid over nanostructured Ru-TiO_2 catalysts," *RSC Advances,* vol. 6, no. 48, pp. 42297-42306, 2016.

[42] O. Mekasuwandumrong, S. Phothakwanpracha, B. Jongsomjit, A. Shotipruk, and J. Panpranot, "Influence of flame conditions on the dispersion of Pd on the flame spray-derived Pd/TiO_2 nanoparticles," *Powder Technology,* vol. 210, no. 3, pp. 328-331, 2011.

[43] J. Morère, M. J. Torralvo, C. Pando, J. A. R. Renuncio, and A. Cabañas, "Supercritical fluid deposition of Ru nanoparticles onto SiO_2 SBA-15 as a sustainable method to prepare selective hydrogenation catalysts," *RSC Advances,* vol. 5, no. 49, pp. 38880-38891, 2015.

[44] K. Y. Jung and S. B. Park, "Anatase-phase titania: preparation by embedding silica and photocatalytic activity for the decomposition of trichloroethylene," *Journal of Photochemistry and Photobiology A: Chemistry,* vol. 127, pp. 117-122, 1999.

[45] E. Truszkiewicz, K. Zegadło, D. Wojda, B. Mierzwa, and L. Kępiński, "The Effect of the Ruthenium Crystallite Size on the Activity of Ru/Carbon Systems in CO Methanation," *Topics in Catalysis,* vol. 60, no. 17-18, pp. 1299-1305, 2017.

[46] M. Martos, B. Julián, H. Dehouli, D. Gourier, E. Cordoncillo, and P. Escribano, "Synthesis and characterization of Ti_1–2xNbxNixO_2–x/2 solid solutions," *Journal of Solid State Chemistry,* vol. 180, no. 2, pp. 679-687, 2007.

[47] M. J. Taylor *et al.*, "Highly selective hydrogenation of furfural over supported Pt nanoparticles under mild conditions," *Applied Catalysis B: Environmental,* vol. 180, pp. 580-585, 2016.

[48] L. Liu, H. Lou, and M. Chen, "Selective hydrogenation of furfural to tetrahydrofurfuryl alcohol over Ni/CNTs and bimetallic Cu Ni/CNTs catalysts," *International Journal of Hydrogen Energy,* vol. 41, no. 33, pp. 14721-14731, 2016.

[49] M. M. Islam, M. Calatayud, and G. Pacchioni, "Hydrogen Adsorption and Diffusion on the Anatase TiO_2(101) Surface: A First-Principles Investigation," *The Journal of Physical Chemistry C,* vol. 115, no. 14, pp. 6809-6814, 2011.

[50] U. Aschauer and A. Selloni, "Hydrogen interaction with the anatase TiO_2(101) surface," *Phys Chem Chem Phys,* vol. 14, no. 48, pp. 16595-602, Dec 28 2012.

[51] Y. Ito, H. Kawamoto, and S. Saka, "Efficient and selective hydrogenation of aqueous acetic acid on Ru–Sn/TiO_2 for bioethanol production from lignocellulosics," *Fuel,* vol. 178, pp. 118-123, 2016.

[52] R. Liu *et al.*, "Physically and chemically mixed TiO_2-supported Pd and Au catalysts: unexpected synergistic effects on selective hydrogenation of citral in supercritical CO_2," *Journal of Catalysis,* vol. 269, no. 1, pp. 191-200, 2010.

[53] F. Wang *et al.*, "Catalytic behavior of supported Ru nanoparticles on the (101) and (001) facets of anatase TiO_2," *RSC Advances,* vol. 4, no. 21, 2014.

[54] N. Aranda-Pérez, M. P. Ruiz, J. Echave, and J. Faria, "Enhanced activity and stability of Ru-TiO_2 rutile for liquid phase ketonization," *Applied Catalysis A: General,* vol. 531, pp. 106-118, 2017.

[55] Y. Liu, Y. Wang, H. Wang, and Z. Wu, "Catalytic oxidation of gas-phase mercury over Co/TiO_2 catalysts prepared by sol–gel method," *Catalysis Communications,* vol. 12, no. 14, pp. 1291-1294, 2011.

[56] F.-C. Duh, D.-S. Lee, and Y.-W. Chen, "Au/CuO_x-TiO_2 Catalysts for CO Oxidation at Low Temperature," *Modern Research in Catalysis,* vol. 02, no. 01, pp. 1-8, 2013.

[57] S. Ali, N. A. Mohd Zabidi, and D. Subbarao, "Correlation between Fischer-Tropsch catalytic activity and composition of catalysts," *Chem Cent J,* vol. 5, p. 68, Nov 3 2011.

[58] D. Lu *et al.*, "RuCo NPs supported on MIL-96(Al) as highly active catalysts for the hydrolysis of ammonia borane," *Journal of Alloys and Compounds,* vol. 694, pp. 662-671, 2017.

[59] A. Ljiljana, C. David, and A. Radoslav, "XPS and STEM study of the interface formation between ultra-thin Ru and Ir OER catalyst layers and perylene red support whiskers," *Journal of the Serbian Chemical Society,* vol. 78, no. 12, pp. 1993-2005, 2013.

[60] V. Matolın, V. Johanek, I. Stara, N. Tsud, and K. Veltruska, "XPS, ISS and TDS study of bimetallic interaction between Pd and Al:CO interaction with supported Pd/alumina catalysts," *Surface Science,* vol. 507-510, pp. 803-807, 202.

[61] L. Zhu *et al.*, "Decoration of Co/Co_3O_4 nanoparticles with Ru nanoclusters: a new strategy for design of highly active hydrogenation," *Journal of Materials Chemistry A,* vol. 3, no. 22, pp. 11716-11719, 2015.

[62] D. Cabaleiro, M. J. Pastoriza-Gallego, C. Gracia-Fernández, M. M. Piñeiro, and L. Lugo, "Rheological and volumetric properties of TiO_2-ethylene glycol nanofluids," *Nanoscale Research Letters,* vol. 8, p. 286, 2013.

[63] H. Kusaka, Y. Hara, M. Onuki, T. Akai, and M. Okuda, "Characterization and Nitrile Group Hydrogenation Study of Supported and Unsupported Ru–Co Catalyst," *JOURNAL OF CATALYSIS,* vol. 161, pp. 96-106, 1996.

[64] F. Wang, Y. Wang, Y. Zhang, Y. Luo, and H. Zhu, "Highly dispersed RuCo bimetallic nanoparticles supported on carbon black: enhanced catalytic activity for hydrogen generation from $NaBH_4$ methanolysis," *Journal of Materials Science,* vol. 53, no. 9, pp. 6831-6841, 2018

APPENDIX

APPENDIX A

CALCULATION FOR CATALYST PREPARATION

The calculation of monometallic 1.5 wt%Ru/TiO_2 catalysts and bimetallic 1.5 wt%Ru with 0.2-0.8 wt%Co/TiO_2 catalysts prepared by incipient wetness impregnation method were shown below. In this work, 2 g of the TiO_2 supports were used for all preparation and determined based on 100 g of catalyst used.

1. Ruthenium(III) nitrosylnitrate solution, Ru 1.5% w/v

   $Ru(NO)(NO_3)_3$ MW. = 317.09 g/mol

2. Cobalt naphthenate, Co in mineral spirits 6%wt

   $CoC_{22}H_{14}O_4$ MW. = 401.02g/mol

Calculation of monometallic 1.5 wt%Ru/TiO_2 catalysts:

TiO_2	100-1.5 = 98.5 g
Ruthenium	1.5 g
For TiO_2	2 g
Ruthenium required	= (2*1.5)/100 = 0.03 g
TiO_2 required	= 2-0.03 = 1.97 g

Ruthenium(III) nitrosylnitrate solution, which Ru precursor was appeared in solution

Ru required in precursor = required Ru of weight ÷ concentration of solution

= 0.03 g ÷ Ru 1.5% w/v

$$= 0.03\ g \times \frac{100\ ml\ solution}{Ru\ 1.5\ g}$$

= 2 ml solution

Calculation of bimetallic 1.5 wt%Ru with 0.2-0.8 wt%Co/TiO_2 catalysts:

For 1.5 wt%Ru-0.2wt%Co/TiO_2

TiO_2	100-1.5 = 98.5 g
Ruthenium	1.5 g
Cobalt	0.2 g
For TiO_2	2 g
Ruthenium required	= (2*1.5)/100 = 0.03 g
Cobalt required	= (2*0.2)/100 = 0.004 g
TiO_2 required	= 2-0.034 = 1.966 g

Ruthenium(III) nitrosylnitrate solution, which Ru precursor was appeared in solution

Ru required in precursor = required Ru of weight ÷ concentration of solution

= 0.03 g ÷ Ru 1.5% w/v

$$= 0.03\ g \times \frac{100\ ml\ solution}{Ru\ 1.5\ g}$$

= 2 ml solution

Cobalt naphthenate solution, which Co precursor was appeared in solution

Co required in precursor = required Co of weight ÷ purity

= 0.004 g ÷ Co 6%

$$= 0.004\ g \times \frac{100\ g}{6\ g}$$

= 0.067 g of Co required

Co required in volume = Co required in precursor ÷ density

$$= 0.067\ g \times \frac{1\ ml}{0.921\ g}$$

= 0.072 ml solution

.

APPENDIX B

CALCULATION OF THE CRYSTALLITE SIZE

Calculation of the crystallite size by using Debye-Scherrer's equation

The crystallite size was calculated from the width at half of height (or full-width-half-max) of diffraction peak of the XRD pattern by using the Debye-Scherrer's equation.

From Scherrer equation

$$D = \frac{K\lambda}{\beta cos\theta}$$

Where D = Crystallite size, A°

K = Crystallite-shape factor or Scherrer constant depanding on shape of crystal (0.9 for FWHM of spherical crystals with cubic symmetry)

λ = X-ray wavelength, (1.5418 A° for CuK_{α})

θ = Observed peak angle, degree

β = X-ray diffraction broadening, radian

X-ray diffraction broadening (β) is the corrected width of a powder diffraction free from all broadening due to the instrument. The α-alumina was used as a standard sample to observe the instrumental broadening data. The most common correction for the X-ray diffraction broadening (β) can be obtained by

From Warren's formula:

$$\beta = \sqrt{B_m^2 - B_s^2}$$

Where B_M = The measured peak width in radians at half peak height

B_S = The corresponding width of the standard material

Exanple: Calculation of the crystallite size of anatase TiO_2

The major peak of anatase TiO_2 was observed at 2θ = 25.42°

The half-height width of the diffraction peak at 25.42° = 0.38

$$= \frac{2\pi \times 0.38}{360}$$

= 0.0066 radian

Corresponding the half-height width of α-alumina of the diffraction peak at 25.42° = 0.0041 radian (B_S)

$$\beta = \sqrt{B_m^2 - B_s^2}$$

$$= \sqrt{0.0066^2 - 0.0041^2}$$

= 0.0051 radian

Thus,

K = 0.9

λ = 1.5418 A° for CuK_α

θ = 25.42/2 = 12.71

β = 0.0051 radian

$$D = \frac{K\lambda}{\beta cos\theta}$$

$$D = \frac{0.9 \times 1.5418}{0.0051 \times \cos 12.71}$$

D = 279 A°

D = 27.9 nm

APPENDIX C

CALCULATION OF THE PHASE COMPOSITION

The fraction of crystal phase of TiO_2 was determined from X-ray diffraction.

The phase composition of TiO_2 was calculated by using the following equation:

$$W_R = \frac{1}{0.884 \times \frac{A}{R} + 1} \times 100$$

Where W_R = the percentage of rutile

A = the peak area of anatase TiO_2 at (101)

R = the peak area of rutile TiO_2 at (101)

The number of 0.884 is the coefficient of scattering

Exanple: Calculation of phase composition of TiO_2

From, $$W_R = \frac{1}{0.884 \times \frac{A}{R} + 1} \times 100$$

$$W_R = \frac{1}{0.884 \times \frac{172}{6} + 1} \times 100$$

$W_R \approx 4\%$

$W_A \approx 96\%$

APPENDIX D

CALCULATION FOR METAL ACTIVE SITE AND DISPERSION

Calculation of Ru active site and Ru dispersion of the catalyst by CO-chemisorption is as follows:

Volume of CO adsorption on catalyst, Vads = $\frac{\mathbf{V_{inj}}}{\mathbf{m}} \times \sum_{\mathbf{i-1}}^{\mathbf{n}}(1 - \frac{\mathbf{Ai}}{\mathbf{Af}})$

Where Vinj = volume injected, 0.02 cm^3

m = mass of catalyst used, g

A_i = area of peak i

A_f = area of last peak

<u>Ru active sites</u>

Ru active site = $S_f \times \frac{\mathbf{V_{ads}}}{\mathbf{Vg}} \times N_A$

Where S_f = stoichiometer factor, CO adsorbed on Ru, CO : Ru = 1

V_{ads} = volume adsorbed

V_g = molar volume of gas at STP, 22414 cm^2/mol

N_A = Avogadro's number, 6.023×10^{23} molecules/mol

<u>Metal dispersion</u>

Metal dispersion % = $100 \times \frac{\mathbf{molecule\ of\ Ru\ loaded}}{\mathbf{molecule\ of\ Ru\ from\ CO\ adsorption}}$

%dispersion = $S_f \times \frac{\mathbf{V_{ads}}}{\mathbf{Vg}} \times \frac{\mathbf{M.W.}}{\mathbf{\%M}} \times 100\% \times 100\%$

Where S_f = stoichiometer factor, CO adsorbed on Ru, CO : Ru = 1

V_{ads} = volume adsorbed

V_g = molar volume of gas at STP, 22414 cm^2/mol

M.W. = molecular weight of the metal

%M = %metal

APPENDIX E

CALCULATION OF FURFURAL CONVERSION AND SELECTIVITY

The catalysts performance for the furfural hydrogenation are shown in this below. Reaction result from GC-FID, found that two peaks product consisted of furfuryl alcohol peak and solvent product peak.

$$\%\text{Conversion} = \frac{\text{Mole in} - \text{mole out}}{\text{Mole in}} \times 100$$

$$\%\text{Selectivity} = \frac{\text{Mole of product}}{\text{Mole of converted reactant}} \times 100$$

Example:

$$\%\text{Conversion of furfural} = \frac{\text{Mole of furfural in} - \text{mole of furfural out}}{\text{Mole of furfural in}} \times 100$$

$$\%\text{Selectivity of furfuryl alcohol} = \frac{\text{Mole of furfuryl alcohol}}{\text{Mole of furfural converted}} \times 100$$

%Selectivity of solvent product = 100 - %Selectivity of furfuryl alcohol

The calibration curve of furfural and furfuryl alcohol are shown in Fig. E.1-E.2

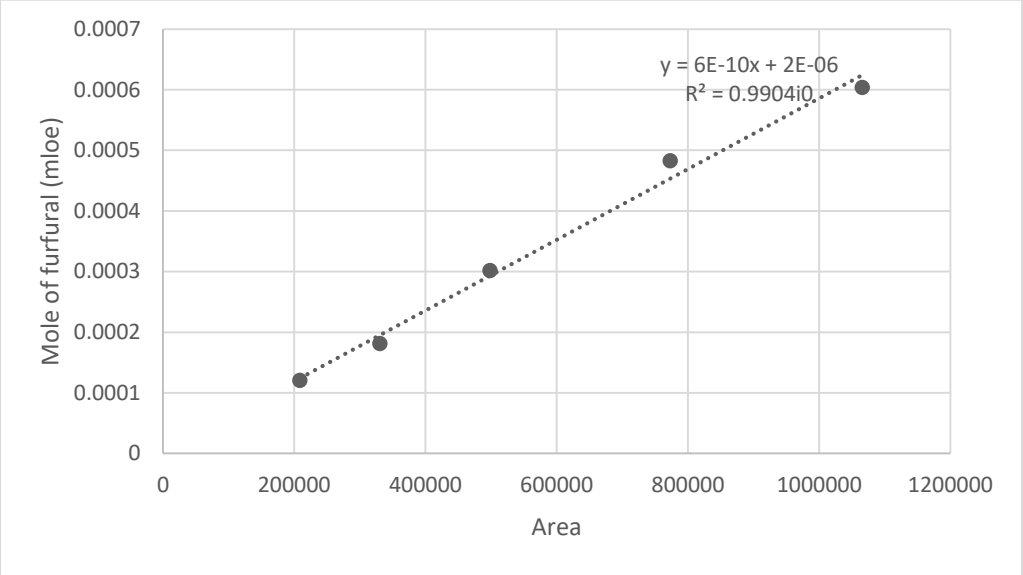

Figure E.1 The calibration curve of furfural

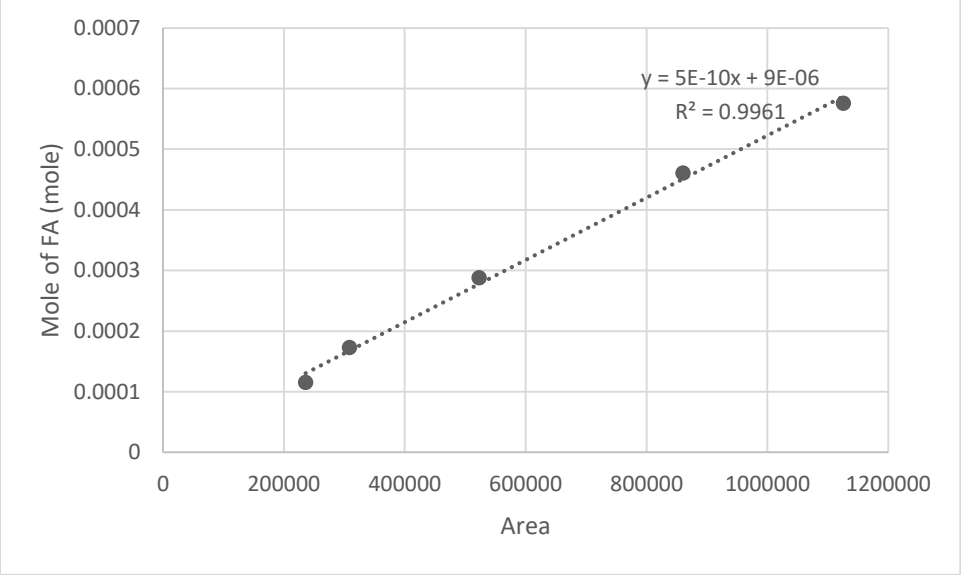

Figure E.2 The calibration curve of furfuryl alcohol

VITA

Mr. Natdanai Nanthasanti was born on October 13th, 1993 in Bangkok, Thailand. He finished high school from Watsuthiwararam School, Bangkok in 2012. He received the Bachelor's Degree of Engineering in Chemical Engineering from King Mongkut's University of Technology Thonburi, Bangkok in 2016. Afterward, he entered to study in Master's Degree of Chemical Engineering at Department of Chemical Engineering program in center of excellence on catalysis and catalytic reaction engineering research group, Chulalongkorn University, Bangkok since 2016.